Spring 2024

Synthesis of an anti-lysozyme antibody tagged with gold or silver nanoparticle for faster western blot

Harunobu Kato
hkato@skidmore.edu

Synthesis of an anti-lysozyme antibody tagged with gold or silver nanoparticle for faster western blot

By Haru Kato

Skidmore college

Senior Thesis, 2024

ABSTRACT

Western blot is an important protein analysis assay enabling protein detection by visualizing the antibody specific antigen-antibody interaction. As a commonly used assay, western blot is taught in upper-level biochemistry and molecular biology students. However, due to its exhaustive process and high cost of antibodies, a modification to western blot is proposed using gold or silver nanoparticles as a tag to the primary antibody for lysozyme. In this experiment, invisible anti-lysozyme antibodies were conjugated to colloidal gold and silver nanoparticles via photochemical immobilization technique, effectively facilitating a physically observable band on the western blot. To eliminate false positives by interactions between immobilized proteins and the nanoparticles, exposed surfaces of metal were covered with different passivating molecules, of those denatured protein show the most promising results. Gold nanoparticles were modeled for silver nanoparticle tags due to its superior stability in buffers compared to its silver counterpart. However, silver nanoparticles are more convenient due to their ease of synthesis and cost advantages. Both gold and silver labeled antibody enables cost and time optimization to western blot as it does not require a secondary antibody nor developer like horse radish peroxidase.

Table of Contents

List of figures

Chapter I. INTRODUCTION

Section 1.1. Motivation

Gold and Silver nanoparticles (AuNP and AgNP) have long been in use including biosensors and bactericidal agents for their ease of synthesis and tunable optical and chemical properties *(1, 2)*. In this work, we took advantage of the optical properties of the nanoparticles by using them as tags for antibodies in western blot. Since its inception, western blot has been used in most fields requiring protein detection and purification. As an essential assay, western blotting is taught in many upper-level biochemistry undergraduate settings not only for the development of lab skills but also to demonstrate the structural and sequential importance of proteins for the interaction between the antigen and antibodies. However, although powerful, western blot is prone to troubleshooting due to its delicate nature and entails high costs and laborious incubation times.

Nanoparticles and their use as biosensors have been especially relevant, exemplified by the frequent use of point-of-care lateral flow assays during the SARS-CoV-2 outbreak *(3-6)*. The unique properties of AuNPs and AgNPs as sensors rise from their localized surface plasmon resonance (LSPR) falling in the visible spectra, in which their color associated max absorbance can easily be measured with a UV-vis spectrophotometer. Both AuNP and AgNP have been used as sensors in lateral flow assays and other detection techniques demonstrating the specificity and low detection limits *(7)*.

Section 1.2. Western blot

Western blot is a protein analysis assay enabling protein detection via antigen-antibody interaction *(8-10)*. The detection of the target antigen is facilitated by the specificity of the antibody to the target antigen. As shown in **Figure 1.1**, first a mixture of proteins (either purified or standard) with the target protein is denatured and separated by size with sodium dodecyl sulfate polyacrylamide gel electrophoresis (SDS-PAGE, **Figure 1.1** row 1). The separated proteins on the gel are transferred to a membrane producing invisible bands, representing proteins of a specific size (**Figure 1.1** row 2). The proteins, now transferred to a solid support, are incubated with the primary antibody specific for the antigen/protein of interest *(8, 9)*. Once excess primary antibody is washed off, an HRP conjugated secondary antibody specific to the primary antibody is added for visualization of the protein band (**Figure 1.1** row 3). In addition to being a protein detection method, western blot is also a semi quantitative assay where the concentration and size of the protein in the mixture can be estimated from the thickness and location of the band if compared to a standard *(8, 10)*.

Although very powerful and commonly used, the entire assay can take up to 6 hours making the process laborious and time consuming. However, this technique is unavoidable in protein detection as it is not only used in research but also in the medical setting, including but not limited to Lyme disease and HIV-1 *(11, 12)*. This makes learning and streamlining the western blot crucial for upper-level biochemistry students in undergraduate colleges and universities. In this work, we tagged an anti-lysozyme antibody with easily synthesized gold or silver nanoparticles (AuNP/AgNP), effectively facilitating a visually observable band on the western blot. By tagging the primary antibody with AuNP

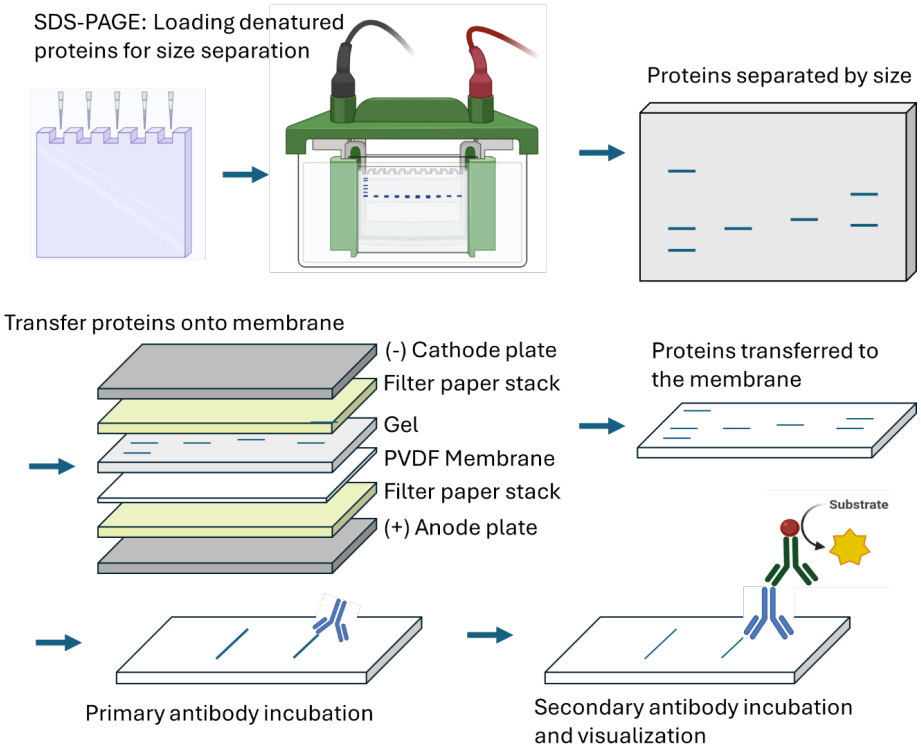

***Figure 1.1. Scheme of SDS-PAGE, transfer, and western blot**, with semidry electrotransfer to PVDF membranes, and final western blot.*

or AgNPs that can be synthesized in most high school and university laboratories, the secondary antibody can be omitted for the detection of the primary antibody-antigen interaction, thus streamlining the process.

Section 1.3. Gold and Silver Nanoparticles as biological sensors

The color of the nanoparticles are governed by the localized surface plasmon resonance (LSPR). Because the size of the nanoparticle is smaller than that of electromagnetic radiation in the visible range, surface electrons of noble metal nanoparticles can absorb visible light to oscillate, a process called resonance *(13, 14)*.

LSPR, typically measured by a UV-vis spectrophotometer, is determined by the element, size, and shape of the nanoparticle. More importantly, LSPR is sensitive to changes in the local dielectric environment surrounding the nanoparticles, in other words, the color of nanoparticles changes when their surrounding molecules change *(14-16)*. Thus, metal nanoparticles can be used in biological processes both as a tag of a biomolecule, when only the location of the color is monitored, or as color changing reporters, correlating to a change in the environment of the nanoparticle.

AuNPs are ideal as biological tags due to their stability in vivo, exemplified in SARS-CoV-2 laminal flow assays *(17-20)*, as a biomarker for prostate cancer diagnosis *(21-23)*, and many other proteins in serum, blood, and saline with aid from other instruments *(24)*. AgNPs are used less in biomedical applications, mainly due to the lack of mechanical studies on the long-term safety of AgNPs on human health *(25)*. The concern in safety is mainly due to the less stable nature of AgNPs compared to AuNPs in biological contexts. However, AgNPs as a tag for the primary antibodies were also explored due to the even more facile synthesis compared to AuNPs as well as the possibility of detecting multiple antigens in one single experiment *(7, 26)*. This is due to AgNPs having a more tunable LSPR resulting in facile synthesis of AgNPs with differing colors. For instance, Yen al., have created a rapid point-of-care laminal flow assay for the simultaneous screening of Dengue, Yellow Fever, and the Ebola Virus with different colored AgNPs for the visualization of each antibody and antigen interaction *(7)*.

Section 1.4. Photochemical Immobilization technique.

Currently, there are many chemical and electrostatic methods of tagging antibodies with AuNP, AgNP, and gold sheet biosensors *(2, 22, 27-31)*. These methods are based on chemical synthesis; consequently, these methods can be complex, time consuming, and hazardous especially for an undergraduate level laboratory exercise. In this work, a Photochemical Immobilization Technique (PIT) was used to irradiate antibodies with UV light, and the subsequent activated antibodies were directly attached to the nanoparticles *(32-34)*. This technique involves the breakage of selected disulfide bridges in the hinge region of the antibody which are induced by the absorption of UV light by nearby tryptophan residues (**Figure 1.2**). The chemically inaccessible disulfide bridges become

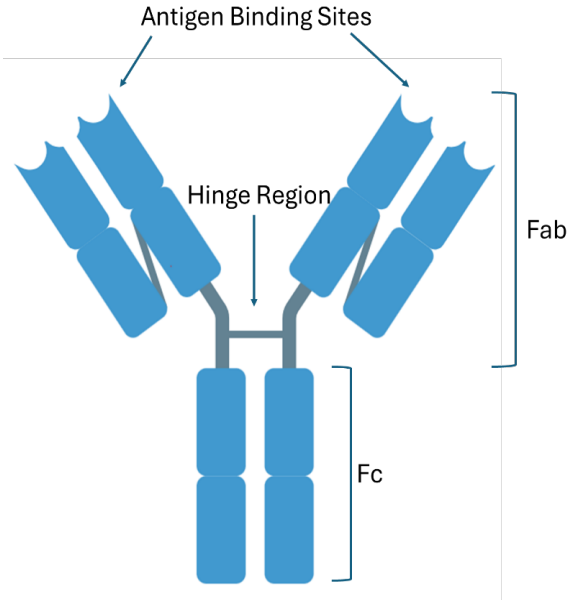

Figure 1.2 Structure of antibody *with antibody binding fragment (Fab) and crystallizable fragment (Fc).*

exposed sulfhydryl groups *(33)*, in which the high affinity between sulfhydryl groups and AuNP or AgNP are used to selectively attach the antibodies to the nanoparticles.

Many biosensors utilizing AuNPs and gold sheets have proved the use of PIT, by functionalizing the sensors with the antibodies in an upright position with the Fab region available for antigen binding *(17, 33-42)*. These silver and gold nanoparticle labeled antibodies can confer cost and time optimization as it does not require a secondary antibody or color-developing reaction like horse radish peroxidase.

Section 1.5 Challenges and Significance

Although many modified western blots exist, most either lack specific descriptions to describe the science behind certain reagents and solvents or utilize specialized equipment or undesirable chemicals for the visualizations and optimization processes of western blot *(27, 43)*. For example, an ultra-high-speed western blot proposed by Higashi et al., is achieved via cyclic draining and replenishing of the antibody solution. Although extremely efficient, the modification requires a hybridization oven and immunoreaction enhancing agents *(43)*. Additionally, most commercially sold western blot kits do not describe the contents of what is included in their solutions and solvents. Although it is understandable for companies to protect proprietary knowledge, not understanding the functions and properties of solvents and buffers does not aid the learning process for students learning about the relevance and value of western blot.

The function of the primary antibody is to selectively detect the antigen via the Fab region, leaving the Fc region available to bind the secondary antibody. The secondary

antibody is generally modified with horse radish peroxidase (HRP) enzyme, which produces a purple color upon reaction with a colorant like 4-chloronaphthol. Because multiple secondary antibodies can bind to one primary antibody, the sensitivity can be increased as multiple HRP conjugated antibodies will amplify the signal compared to one. Other works that have tried to shorten the time of western blot, tag the primary antibody with more sensitive labels such as fluorescence *(44)*. Another difficulty of labeling the primary antibody is that it must be done via a chemical reaction and then purified *(45)*. Commercially, ThermoFisher offers a fast chemiluminescence kit for 1-hour western blot; not only is this proprietary knowledge, but it is specific only to certain antibodies.

AuNP and AgNP tags for antibodies require specific stabilizing surface molecules or ligands on the surface or metal nanoparticles to prevent aggregation or reshaping. These molecules can be displaced during the many different steps of western blot. Other groups have demonstrated that it is possible to label antibodies with nanoparticles, while maintaining the specificity of the antibody. *(17, 28, 33, 46)* Thus, optimization of the environment and buffer conditions is required to ensure only the antibody is interacting with the antigen and not the nanoparticles with the antigen. By attaching colloidal AuNP or AgNP to antibodies, optimization of western blot is achieved thus improving the learning process of western blot as all buffer conditions and functions of molecules are known. By optimizing the labor and cost required for western blot, this modified western blot utilizing nanoparticles can improve the time constraint and logistical issues. In this work, anti-lysozyme antibody tagged with gold nanoparticle (Ab-AuNP) or silver nanoparticle (Ab-AgNP) were synthesized, effectively facilitating a visual band on the western blot membrane.

Section 1.6. Specific aims

AuNP and AgNP and their optical properties have been used for decades with various applications, including the detection of proteins of interest. In this work, a modified western blot is proposed by attaching colloidal gold or silver nanoparticles to primary antibodies, facilitating a physically observable band on the western blot. AuNP was experimented on first as a model tag for AgNP due to its frequent use in protein detection and other point of care laminal flow assays *(1, 2)*. Additionally, AuNPs have superior stability in biological buffers, but more laborious synthesis compared to AgNP.

In this work, the invisible antibody was tagged with a colloidal noble nanoparticle. Once conjugated, the free surfaces on the nanoparticle were blocked (passivated) to ensure both stability and specificity by the antigen-antibody interaction and not between the nanoparticle and the antigen. In addition to passivation, preservation of nanoparticle shape and color was explored as a dark color will enable easier detection on the white background of the blot. Primary antibodies tagged with gold (Ab-AuNP) or silver (Ab-AgNP) nanoparticles enable cost and time optimizations as they do not require a secondary antibody or color-developing reactions like horse radish peroxidase. These modifications to the primary antibody make the western blot assay more accessible to upper-level undergraduate biochemistry students.

Aim 1. Tagging the invisible antibody with colloidal noble nanoparticles.

To conjugate the antibody and nanoparticle, the high affinity between the thiol groups of the antibody and the Au/AgNP were utilized. Although other conjugation techniques were considered, due to this work's intent of use in an undergraduate setting, a

safe and easy-to-use Photochemical Immobilization Technique (PIT) was chosen to conjugate the antibody to the nanoparticles. First, the effectiveness of PIT on the antibody was measured with Ellman's reagent to confirm thiol formation. Then, using the sensitivity of the localized surface plasmon resonance (LSPR) of the Au/AgNP, the conjugation between the antibody and the nanoparticles was measured by changes in the LSPR before and after conjugation.

Aim 2. Adjusting biocompatibility of the nanoparticles in solution

Western blot is carried out in specific buffers, different from the conditions in which metal nanoparticles are prepared. Ideally, the nanoparticles will be stable in the western blot binding buffer, maintaining their shape and LSPR. However, both bare AuNP and AgNP suffered aggregation or reshaping when exposed to western blot binding buffers. Thus, buffer adjustments were made in terms of salt concentrations and detergents.

Aim 3. Isolation of the nanoparticle from the environment

Once conjugation between the noble nanoparticle and the antibody was achieved, free surfaces on the nanoparticles were isolated (passivated) from the environment. This was to ensure AuNPs or AgNPs would not interact with any free thiol groups in the immobilized proteins during the western blot. In addition to bovine serum albumin (BSA), which has been used in the past for passivation of AuNP, other reagents like polyvinyl pyrrolidone (PVP), polyethylene glycol (PEG), 6-mercaptohexanoic acid (MHA), and denatured BSA (dBSA) were considered as passivating agents *(28, 30, 32, 47-49)*.

Aim 4. A western blot with primary antibody tagged with noble metal nanoparticle.

Finally, Ab-AuNP or Ab-AgNPs (both passivated) were tested using the western blot assay for specificity of the antibody as well as detection limits.

Section 1.7. Experimental Approach

Aim 1. Tagging primary antibody to noble metal nanoparticle.

Rationale. Although PIT has been used in previous studies, most of these include laminal flow assays, in solution assays, or instrument assisted assays. As the goal of this work is to be used in an undergraduate setting, facile synthesis, convenience, and safety were taken into consideration. First, the disulfide bridges of the antibody were broken, and free thiol groups were exposed by irradiation with UV-light. Then, the antibody with free thiol groups were mixed with colloidal noble metal nanoparticles.

Methods. *Ellman's reagent*. To validate the formation of free thiol groups, a secondary antibody was irradiated in a quartz cuvette for 1 min by a 253.7 nm germicidal UV-lamp (25 W). The increase in exposed thiol groups were compared against a cystine standard and measured by the increase in absorption by TNB, a product of the reaction between Ellman's reagent (5,5'-Dithio-bis-(2-nitrobenzoic acid)) and the exposed thiol groups *(50, 51)*.

Gold and Silver nanoparticle synthesis. First, gold nanoparticles (AuNP) were synthesized via citrate reduction of gold salt, and silver nanoparticles (AgNP) were synthesized via simultaneous multiple asymmetric reduction technique of silver salts *(16, 52-56)*. The concentrations of metal nanoparticles were obtained using the geometry and

optical properties of the nanoparticles as reported in previous works *(57, 58)*. The size and shape were recorded via transmission electron microscopy (TEM) and the LSPR was measured using a UV-visible spectrophotometer.

Conjugation detection by LSPR. Conjugation of the activated antibodies with the noble metal nanoparticles were measured by observing small shifts in the LSPR of the nanoparticle, based on the sensitivity of the LSPR to changes in the refractive index of the surrounding *(59, 60)*.

Data analysis. The absorbances of the Ellman's reagent added to the cysteine standards and the activated antibody were measured by a UV-visible spectrophotometry. The TEM images of the nanoparticles were analyzed by ImageJ. The LSPR of the nanoparticles were measured by a UV-vis spectrometer and analyzed on excel. The shift in LSPR was calculated after normalizing the spectra to a maximum absorbance of 1.

Potential Limitations and Hazards. Although past literature has noted that PIT conjugates antibodies on the Fc region and not the Fab region, thus only exposing the antigen binding region, LSPR will only measure a bind to the surface of the nanoparticle but will not provide information about the orientation of the antibody.

Aim 2. Adjusting biocompatibility of the nanoparticles in solution

Rationale. Although AuNP were thought to maintain their shape in the biological buffers and water, both AuNP and AgNP were observed to reshape, change in color, or aggregate. Thus, the cause of the reshaping and aggregation of the nanoparticles by the buffer were explored and adjustments were made in terms of salt concentrations and detergents.

Methods. AgNP (1 mL) was added to tris-buffered saline with and without Tween-20, phosphate-buffered saline with and without Tween-20, and 0 to 1.5 mM NaCl. LSPR and color changes were measured to observe shape changes by the AgNP.

Data analysis. The LSPR was measured by UV-visible spectroscopy; shape and size of nanoparticles were measured by TEM as described in Aim 1.

Aim 3. Isolation of the nanoparticle from the environment

Rationale. To isolate free surfaces of AuNP and AgNP from the environment and other proteins, many passivating molecules were considered. Although BSA, PVP, PEG, and MHA have been used in other assays to passivate the nanoparticles *(28, 30, 32, 47-49)*, adjustments were required for the use of the nanoparticles in the western blot assay. To observe the nanoparticle passivation, LSPR and western blots without antibody were utilized. Passivation is necessary to ensure specificity during the western blot, where only the antibody is attached to the antigen.

Methods. The passivation of the nanoparticles was modeled by AuNP. First, the AuNP were exposed to differing concentration and time of BSA, PVP, PEG, MHA, and denatured BSA. Binding to the surface of AuNP was measured by LSPR, where a small increase of LSPR indicates the passivating agents attaching to the nanoparticles. The passivated AuNP without antibody were added to a blot with lysozyme (LYZ) and ovalbumin (OVA) in western blot binding buffer (Tris saline buffer with detergent).

Data analysis. The shift of the LSPR of noble metal nanoparticles were measured and analyzed as described in **aim 1**.

Aim 4. A western blot with primary antibody tagged with noble metal nanoparticle.

Rationale. Under adjusted buffer conditions, anti-lysozyme antibody tagged with passivated gold or silver nanoparticle (Ab-AuNP or Ab-AgNP) was added to a western blot for the final western blot analysis.

Methods. The passivated AuNP or Ab-AuNP were added to an OVA and LYZ immobilized blot. Similarly, passivated AgNP and Ab-AgNP were added to a blot with immobilized OVA, BSA, and LYZ. These experiments measured the effectiveness of passivation, the stability of the nanoparticle, and if the detection of the lysozyme worked as intended.

Data analysis. Blots were matched to SDSPAGE stained with Coomassie blue to identify the bands corresponding to LYZ, BSA, or OVA.

Chapter 2. EXPERIMENTAL WORK

Section 2.1. Reagents and instrumentation

All reagents were purchased and used as received. L-ascorbic acid, gold (III) chloride trihydrate, Tween 20, DTNB (5,5′-dithio-bis-(2-nitrobenzoic acid) / Ellman's reagent), cysteine standard, 6-mercaptohexadecanoic acid (MHA), polyethylene glycol (PEG), ammonium persulfate, tetramethyl ethylenediamine (TEMED), and Coomassie Brilliant Blue G-250 were from Sigma Aldrich; sodium borohydride, sodium citrate dihydrate, sodium chloride, sodium phosphate, ethylenediaminetetraacetic acid (EDTA), hydrochloric acid, acetic acid, nitric acid, methanol, bovine serum albumin (BSA), 40% acrylamide:bisacrylamide were from Fisher Scientific; polyvinyl Pyrrolidone (PVP) M.W. 40,000 g/mol was from Alfa Aesar; Tris was from Santa Cruz chemicals; silver nitrate was from Acros Organics; and electrophoresis 4x loading buffer was from Invitrogen. Primary antibody (rabbit anti-lysozyme) and secondary antibody (goat HRP-conjugated anti-rabbit) were from AVIVA systems biology. Barnstead system was used to obtain ultrapure water.

Transmission Electron Microscopy was done in a Hitachi HT7800 TEM at 120 kV with 40,000 x magnification. The samples of the silver and gold nanoparticles were obtained by depositing 2 µL of particle solutions onto carbon-Formvar coated copper TEM grids and drying in a desiccator. UV-visible spectroscopy was done using an Ocean Optics UV-Vis spectrophotometer with a 1-cm polystyrene cuvette and a HR4000 detector. Measurements of pH were done using a pH meter from Accumet. Protein electrophoresing was done using a Mini-PROTEAN Tetra Cell and gel casting system from Bio-Rad. For western blot, a semi-wet protein transfer apparatus from Pierce was used.

Section 2.2. Syntheses of nanoparticles

Gold Nanoparticle synthesis. AuNP were synthesized via citrate reduction *(16, 53-55)* in aqua regia cleaned glassware. Briefly, 50 mL of 1 mM $HAuCl_4 \cdot 3H_2O$ was refluxed with gentle stirring. After a rolling boil, 5 mL of 38.8 mM Sodium citrate dihydrate solution was quickly added and refluxed for an additional 30 min and allowed to cool to room temperature. The AuNP were stored in brown bottles in the dark until further use. The concentration of AuNP was calculated using Haiss' supplemental section *(57)*.

Silver Nanoparticle synthesis. AgNP were synthesized by a single-pot experiment in nitric acid washed glassware *(56, 58)*. Briefly, 100 mL of 0.18 mM $AgNO_3$ and 0.145 mM polyvinylpyrrolidone were placed a 500 mL Erlenmeyer flask, while swirling 0.1 M ascorbic acid and 0.15 mL of 1 mM sodium borohydride were quickly added. Once the sodium borohydride was added, the swirling was continued for another 10 s to finish the reduction reaction of the silver ions into silver nanoparticles. The solution was left in a dark brown bottle for up to a maximum of 1 week.

Section 2.3. Protein electrophoresis and western blot

This procedure is adapted from the manufacture's manual *(61)*. To prepare 12.5% polyacrylamide gel, the gel casting system was assembled as shown in **Figure 2.1.** Briefly, a separating gel was made by mixing 40 % acrylamide:bisacrylamide (3.125 mL), 1.5 M Tris-HCl pH 8.8 (2.5 mL), 1.25 % SDS (800 µL), ultrapure water (3.465 mL), 10 % Ammonium persulfate (100 µL), and TEMED (10 µL). The mixture was added between the plates, leaving 2 cm clearance from the top of the short plate. After polymerization, the

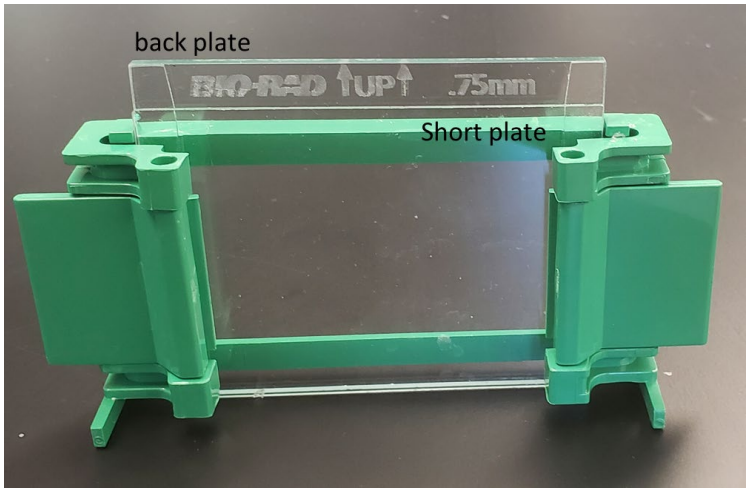

Figure 2.1 Assembled gel casting system.

separating gel was prepared by mixing 40 % acrylamide:bisacrylamide (625 µL), 1 M Tris-HCl pH 6.8 (625 µL), 10 % SDS (50 µL), ultrapure water (3.65 mL), 10 % ammonium persulfate (50 µL) and TEMED (5 µL). The stacking gel mixture was poured on top of the separating gel, then the comb was inserted. The gel was used immediately after polymerization.

Samples were prepared for electrophoresis by loading a protein mixture (1.1 mg/mL lysozyme and 1.8 mg/mL ovalbumin) with 1 X loading buffer (50 mM Tris-HCl pH 6.8, 10 % glycerol, 2 % SDS, 0.0025 % bromophenol blue, 1 % β-mercaptoethanol, 12.5 mM EDTA). The samples were boiled for 5 minutes in a heating block, and 10 µL were loaded in each well of the gel. Protein ladder was prepared as indicated by the manufactures and 10 µL was loaded in each gel. Electrophoresis was run at 130 V for 1 h in Tris-Glycine buffer (25 mM Tris-HCl pH 8.3, 192 mM glycine, 0.1 % SDS). A portion of the gel was stained with Coomassie blue staining solution (0.1 % Coomassie Brilliant Blue G-250 in 10 % methanol and 10 % acetic acid), and destained with 10 % methanol, 10 % acetic acid.

The rest of the gel was used to prepare the blot. Briefly, the gel was washed with ultrapure water for 10 min, then a pre-wetted PVDF membrane (30 seconds in methanol and 2 min in water), four pieces of filter paper and the membrane were equilibrated in transfer buffer (25 mM Tris-HCl pH 8.3, 192 mM glycine, 20 % methanol) by gentle rocking for 10–15 min. The sandwich was assembled with two pieces of paper on the bottom (anode), the membrane on top, then the gel on top of the membrane and finally, two layers of filter paper. Bubbles were removed by rolling a pipette over the top layer. The apparatus was covered with top plate (cathode) and transfer was carried out at 15 V for 30 min.

To carry out western blot, the membrane was blocked with 10 mg/mL BSA in TBST (50 mM Tris-HCl pH 7.6, 150 mM NaCl, 0.05 % Tween-20) for 1 hour at room temperature. The blot was washed twice for 10 minutes each with TBST, incubated in primary antibody conjugated with metal nanoparticles; the blot was gently rocked for up to 1 hour to observe the development of colored bands.

Section 2.4. Antibody activation

Ellman's assay was used to verify the formation of thiols This experimental approach is adapted from assay #22582 by ThermoFisher scientific *(62)*. Ellman's reagent was prepared by dissolving 4 mg of DTNB in 1 mL of PBS / EDTA buffer (0.1 M sodium phosphate, 0.15 M NaCl, 10 mM EDTA pH 7.2). Cystine standards of 18 to 45 µM were prepared in water. Photochemical Immobilization Technique (PIT) was used to activate the antibodies, breaking the disulfide bonds, and freeing the thiol groups *(32)*. Briefly, a solution of 50 µg/mL of antibody was added to a quartz cuvette and irradiated for 1 min

with two 253.7 nm germicidal UV-lamps (25 W) (**Figure 2.2**). Secondary antibody was used to validate PIT. While primary antibody was used to create antibody conjugated with metal nanoparticles.

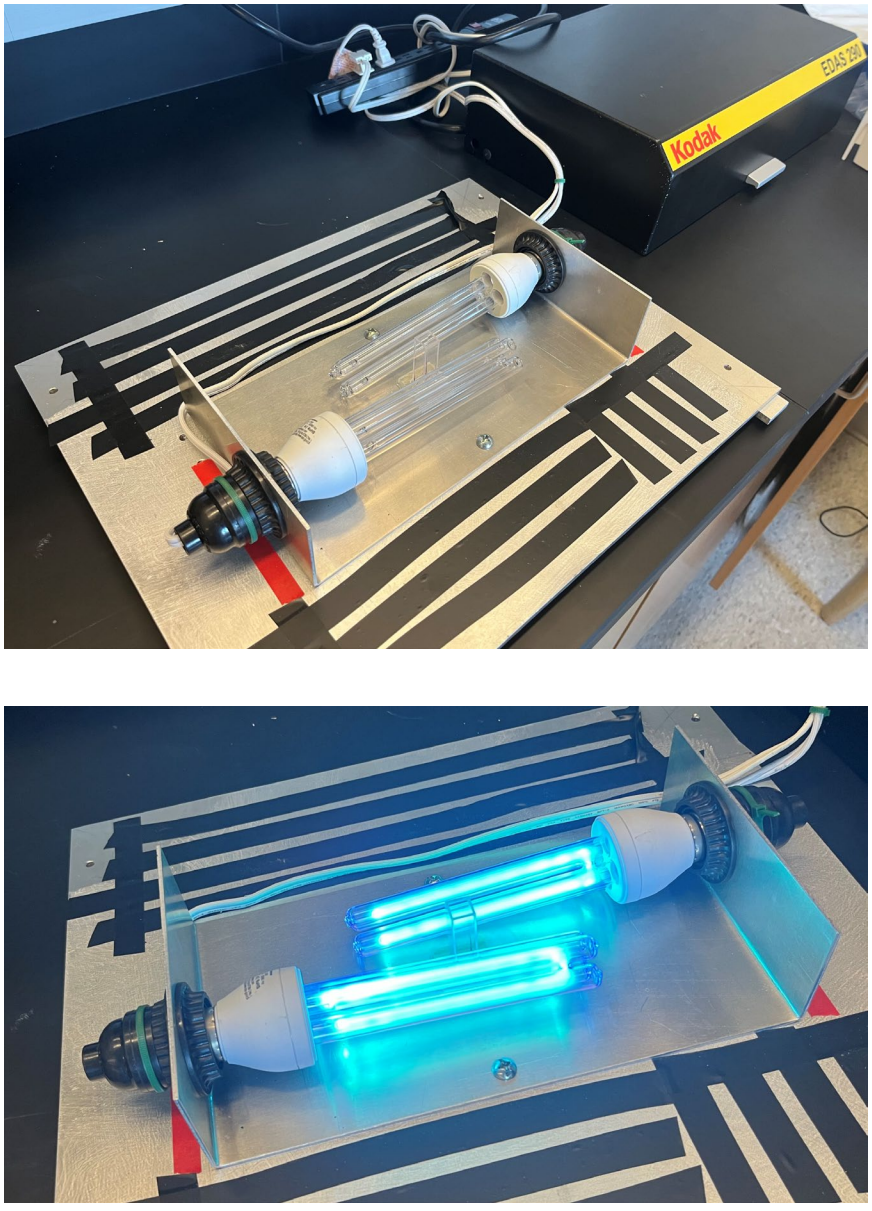

Figure 2.2. PIT, UV-lamp set up. *(top) experimental setup of 2 UV lights with quartz cuvette and black cover to shield user from light. (bottom). Example of UV-light irradiation on sample (black electrical tape is to cover holes in the metal plate, thus minimizing light leakage).*

Section 2.5. Conjugation

For conjugation, AuNP or AgNPs were centrifuged for 10 mins at 12,000 x g and restored in ultrapure water, then a volume of activated antibody solution was added to 3 mL of the centrifuged AuNPs. Conjugation time varied from 5 min to 24 hours. The ratio of antibodies per nanoparticles (#Ab/NP) was calculated by diving the moles of antibodies added to the moles of nanoparticles.

$$\frac{\#Ab}{NP} = \frac{moles\ Ab\ in\ conjugation}{moles\ NP\ in\ conjugation}$$

Considering that anti-lysozyme antibody is obtained as a lyophilized powder to be restored in 2 mL of ultrapure water to produce an 80 mg/mL stock, using a molar mass of 150 kg/mol, the concentration of the stock is 0.53 mM. For activation, a volume of the stock (V_s) was diluted in water to a final volume (V_a) and then irradiated with UV-light. For conjugation, an aliquot of activated antibody was taken for conjugation (V_c) and added to a volume of metal nanoparticles (V_{NP}). Considering all these steps, the moles of antibodies and nanoparticles in the final conjugation volume is calculated using the following equations:

$$moles\ Ab\ in\ conjugation\ = 0.53x10^{-3}\ \frac{mol}{L} * \left(\frac{\mu L\ of\ V_s}{\mu L\ of\ V_a}\right) * \frac{\mu L\ of\ V_c}{1x10^6}$$

$$moles\ of\ NP\ in\ conjugation = [NP]\frac{mol}{L} * V_{NP}$$

Section 2.6. Passivation of metal nanoparticles.

Once conjugated with the activated antibody, unless stated otherwise, the metal nanoparticles were isolated from the surrounding environment with passivating agents. The passivating agents were exposed to the metal nanoparticles from 15 min to 24 hours. Experimented passivating agents include bovine serum albumin (BSA, 0.2 % to 1.4%) *(32)*, polyethylene glycol (PEG, 0.2% to 1.5%) *(30, 47)*, polyvinyl pyrrolidone (PVP, 0.2 % to 1.5%) *(48)*, 6-mercaptohexadecanoic acid (MHA, 0.5 to 5 μM) *(49)*, and denatured BSA (dBSA, 0.02 % to 0.15 %).

Section 2.7. Stability of nanoparticles in biochemical buffers.

Synthesized AgNPs were centrifuged for 30 min and added to modified buffers or a sodium chloride solution in a 1 ml:1 ml ratio. The UV-vis spectra of the AgNPs were measured after 30 min, 1 h, and 2 h post exposure to the biochemical buffer or sodium chloride solution. Biochemical buffers used were phosphate buffered saline (PBS, 137 mM NaCl, 2.7 mM KCl, 10 mM Na_2HPO_4, 1.8 mM KH_2PO_4), tris-buffered saline (TBS, 20 mM Tris, 150 mM NaCl), and their counterparts with tween-20 (0.1 % w/v) added (PBST and TBST).

Chapter 3. RESULTS

The goal of this immunoassay is to use gold nanoparticles (AuNP) or silver nanoparticles (AgNP) as visual reporters of the binding between primary antibody (anti-lysozyme) and its antigen (immobilized lysozyme, LYZ). To this end, the primary anti-lysozyme antibody was attached to colloidal nanoparticles (conjugation) forming an antibody tagged with a metal nanoparticle, which was isolated from the environment with blocking agents (passivation). The antibody labeled with metal nanoparticle was incubated with the immobilized antigen until a visual band was observed (western blot).

Figure 3.1 shows the organization of this chapter. First, the antibody (Ab) activation and analysis will be presented since this is used with both nanoparticles (section **3.1**). The studies with AuNP are presented first because these nanoparticles are more stable than AgNP and thus used more in biological assays. For AuNP studies, the results for the synthesis are shown in Section **3.2**, conjugation with primary antibody in Section **3.3**, passivation from the environment in Section **3.4**, and Section **3.4** shows the modified western blot. For the studies with AgNP, the results for the synthesis are shown in Section **3.5**, conjugation with primary antibody in Section **3.6**, stability of AgNP in biochemical buffer in Section **3.7**, and modified western blot in Section **3.8**. The stability of the nanoparticle in the western blot buffers is very important due to the color of the nanoparticle being shape dependent. All the steps culminate into a stable-unreactive AgNP, visually tagging the interaction between the primary antibody and the lysozyme antigen on the blot.

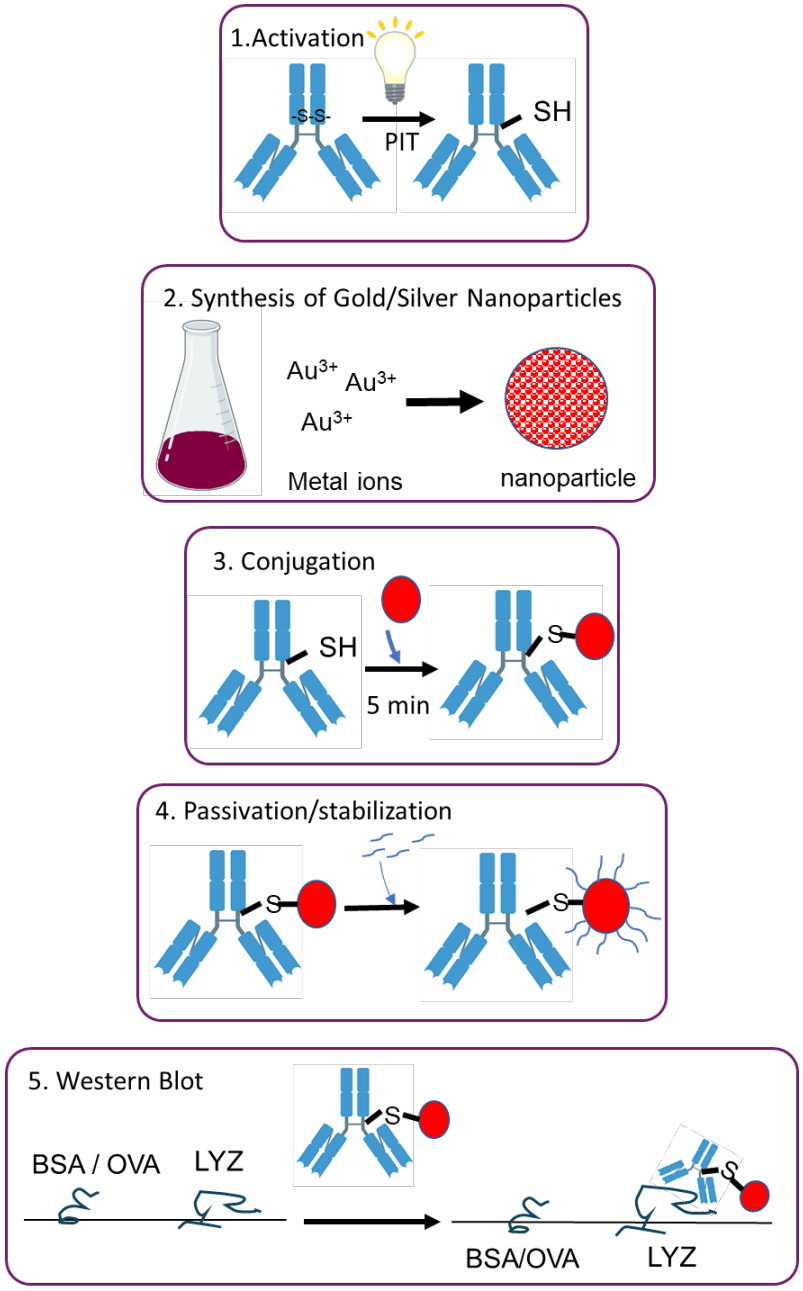

Figure 3.1. Organization of the results section.

Section 3.1. Antibody Activation

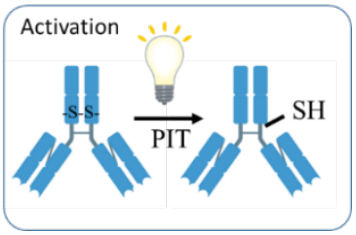

To conjugate the antibody (Ab) to either gold or silver nanoparticles (AuNP/AgNP), the thiol groups contained in the disulfide bridges of the Fab region of the antibody were considered. By utilizing the attraction between the nanoparticles and sulfur, the antibody would be tagged and visualized. This section reports on the findings of breaking the disulfide bonds and exposing free thiols. To expose the thiol groups from the disulfide bridges, a photochemical immobilization technique (PIT) was used *(32, 33)*.

Figure 3.2 summarizes the verification of free thiol formation via PIT using Ellman's assay *(33, 35, 38)*. A calibration with cysteine standard showed that this technique has a limit of detection of 0.25 mM, and an extinction coefficient of 23,250 $M^{-1} \cdot cm^{-1}$ compared to the expected extinction coefficient of 14,510 $M^{-1}cm^{-1}$ (**Figure 3.2 A**) *(50, 51)*. Irradiation conditions of PIT were tested by exposing secondary antibodies to UV-light for 1 minute (**Figure 3.2 B**). When the irradiation was performed with a "cold" lamp, the concentration of thiols was 22 µM (Abs= 0.571), and when the lamp was warmed-up for 15 min a concentration of thiol was 59 µM (Abs=1.387). An un-irradiated control showed the concentration of thiol of 0.2 µM (Abs = 0.008). Because of an increase in concentration of sulfhydryl groups, this result showed that the use of PIT is a facile method of exposing thiol groups for possible use of attaching the activated antibody and the metal nanoparticles.

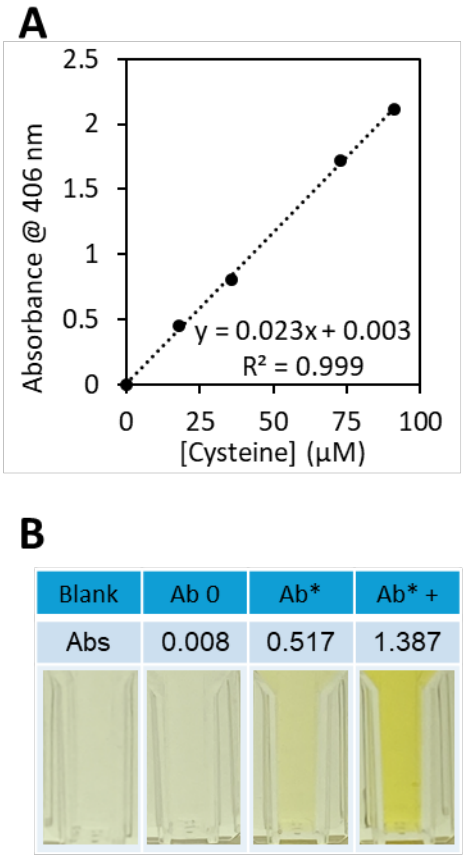

Figure 3.2. Ellman's assay. *(A) Calibration curve. (B) Photographs of Ellman's assay without antibody (Blank), non-irradiated antibody (Ab0), antibody irradiated for 1 min with cold lamp (Ab*), and Antibody irradiated 1 min with pre-warmed lamp (Ab*+). Absorbance was measured at 406 nm.*

Section 3.2. Gold Nanoparticle Synthesis

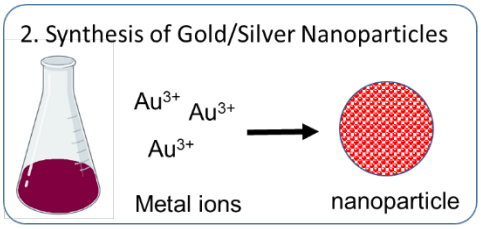

Gold nanoparticles (AuNP) were prepared via reduction with citrate with slight modifications *(16, 53-55)*. Nanoparticles prepared in this way are known to be very reproducible and relatively inert, resulting in 13 nm spheres with LSPR at ~520 nm (**Figure 3.3 A, D**). **Figure 3.3 C** shows the synthesis resulted in uniformly sized AuNPs with LSPR at 522 nm and average size of 13 ± 1 nm. Although the time of reflux during the synthesis of AuNP was longer than described by Roca et al., both the size and LSPR were both very similar in values *(16)*. The characteristics of size, size distribution or uniformity of AuNP sizes, and localized surface plasmon resonance (LSPR) corresponding to the size are all expected based on the trans electron micrographs and UV-vis absorption data. The corresponding LSPR of 522 nm to the size of the nanoparticle (13 ± 1 nm), and size distribution was typical in similar AuNP synthesis methods utilizing citrate reduction method (**Fig. 3.3 D**) *(63)*. Finally, as shown in **Figure 3.3 B**, the synthesized colloidal AuNP solution is a deep red color desirable to for tagging antibody in the western blot.

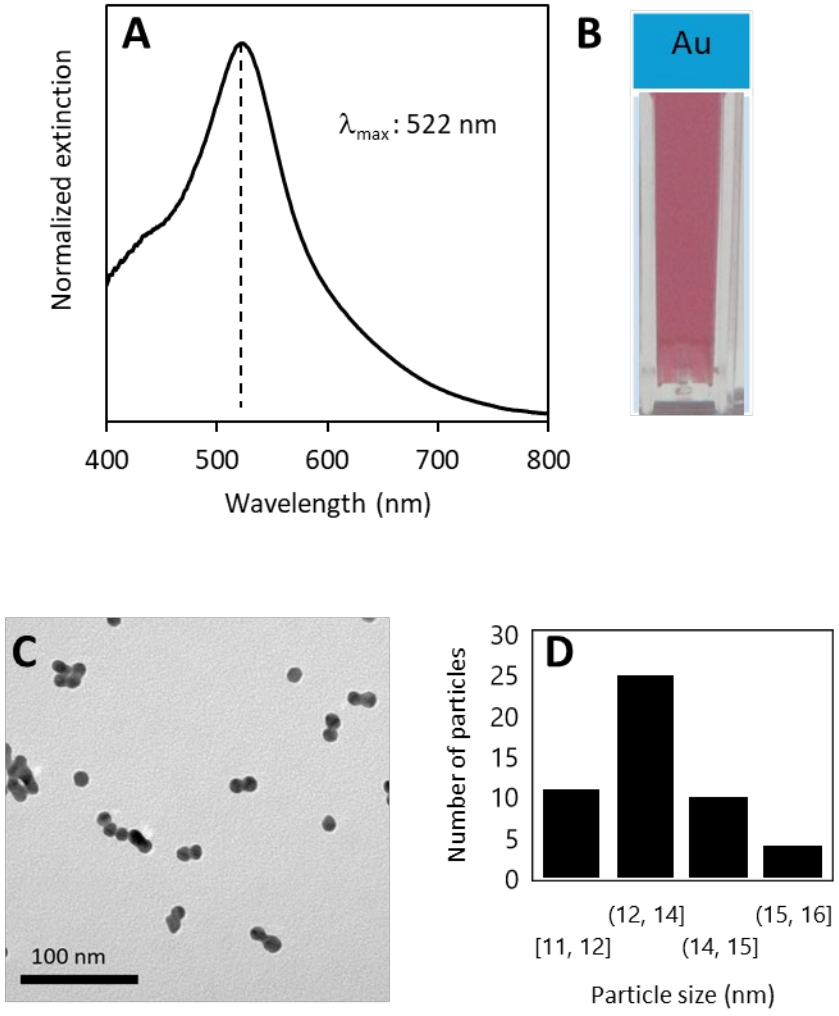

Figure 3.3. Characterization of AuNP. *(A) Extinction spectra and (B) photograph of colloidal AuNP solution in water. (C) Transmission electron micrographs showing the shape and approximate sizes of spherical AuNPs, and (D) histogram showing average size of AuNP = 13 ± 1 nm (n = 51).*

Section 3.3. Gold Nanoparticle Conjugation Study

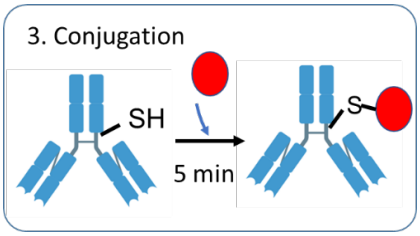

Synthesized gold nanoparticles (AuNP) and activated antibody (Ab*) were incubated together to form an antibody tagged with gold nanoparticles (Ab-AuNP). This conjugation step is crucial towards conferring visual detection of the antigen-antibody interactions between lysozyme and its primary antibody. Two factors were investigated to optimize the conjugation step; the concentration ratio of antibody to nanoparticle and conjugation time. **Figure 3.4** summarizes changes in the optical properties of gold nanoparticles used to monitor conjugation.

The number of antibodies was calculated as explained in **Section 2.6**. The number of nanoparticles was calculated using the average size of nanoparticles obtained via TEM and concentration obtained using Haiss' approach *(57)*. Thus, AuNPs of 13 nm with an absorbance of 0.509 at 450 nm, would have an approximate concentration of 7.2 nM. **Figure 3.4 A** shows that when antibodies are added, the nanoparticle's LSPR shifts toward longer wavelength, showing that the molecules on the surface of the nanoparticles are being exchanged. Thus, implying the antibodies are conjugating on the surface of the nanoparticles. This shift towards longer wavelengths increases as the number of antibodies increases and plateaus after approximately 37 antibodies per nanoparticle (**Figure 3.4 B**). Consequently, further experiments were carried out with concentrations above 37 antibodies per nanoparticle.

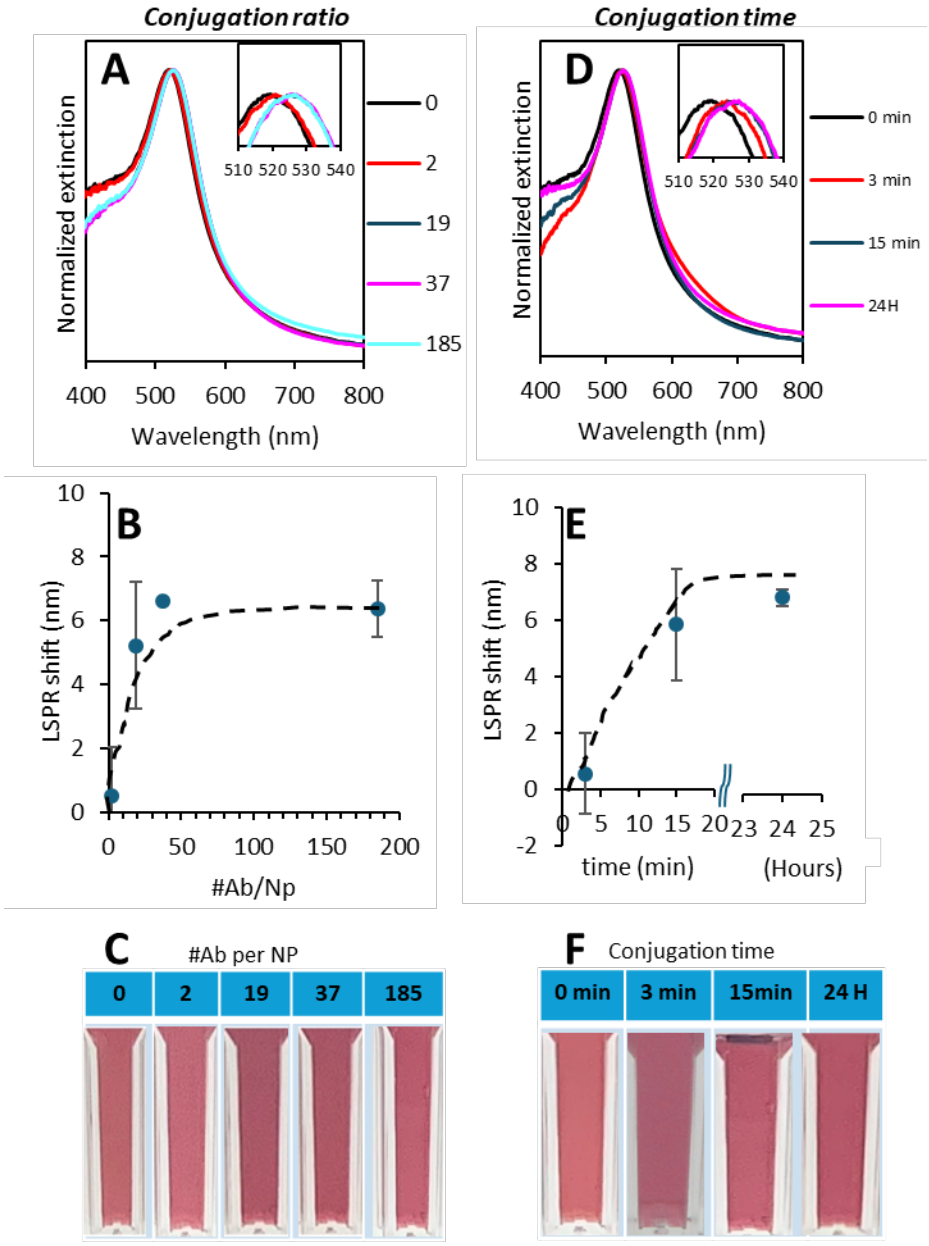

Figure 3.4. Conjugation effect on optical properties of AuNP. *(A) Extinction spectra, (B) LSPR shift dependence and (C) photographs for the studies of conjugation ratio of antibody per nanoparticle. (D) Extinction spectra, (E) LSPR shift dependence and (F) photographs for the studies of conjugation time.*

In addition to antibody to AuNP ratios, the conjugation time was also measured. **Figure 3.4 D and E** show that the LSPR shift increased as the conjugation time was increased from 5 mins to 24 h. Considering the uncertainty of the LSPR shift at 15 min and 24 hours, the difference is not considered significant and future experiments were carried out with a minimum conjugation time of 15 min. Additionally, **Figure 3.4 C and F** show that the preferred deep red color was preserved regardless of Ab to AuNP ratio and conjugation time. For experiments in the undergraduate laboratory, the fastest and most flexible parameter are 15 min conjugation with at least 37 antibodies per 13 nm AuNP.

Section 3.4. Gold Nanoparticle Passivation and Western Blot

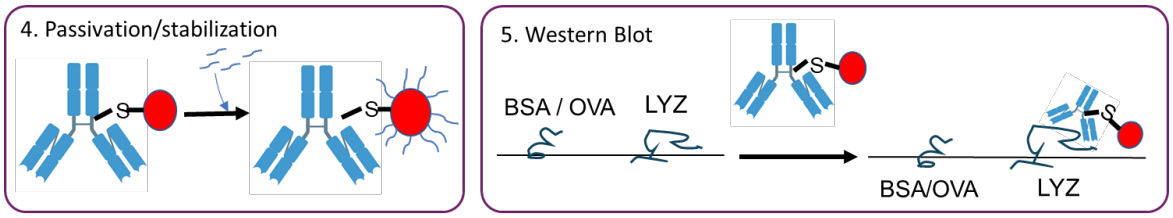

Western blot is based on the binding between the antibody and antigen, carried out in biological buffers. The necessity of passivation rises due to the possibility of false positive results if AuNPs bind the antigen or from the precipitation of nanoparticles. This section addresses the necessity of isolating the AuNP's surface from the environment and the antigen. This ensures that results are observed from the specific interaction between the antibody (anti-lysozyme) and the antigen (immobilized lysozyme) and not from no-specific interactions between the AuNP and the antigen. When added to biological buffers, the bare AuNP's color drastically changed from a deep red to a blue color (**Figure 3.5 B**), which was confirmed by the LSPR shift of ~130 nm towards longer wavelengths, indicating that nanoparticles are aggregating (**Figure 3.5 A**).

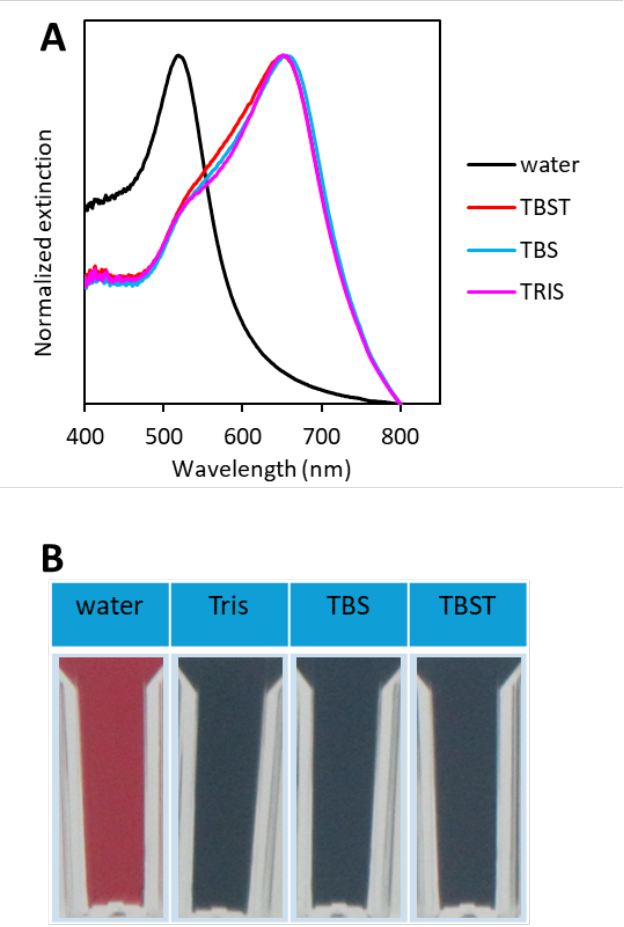

Figure 3.5. Stability of AuNP in buffers. *(A) Extinction spectra and (B) photographs of AuNP solutions in Water, Tris (50 mM, pH 7.6), TBS (50 mM Tris pH 7.6, 150 mM NaCl), and TBST (50 mM Tris pH 7.6, 150 mM NaCl, 0.5% Tween 20).*

The first passivating agent tested was bovine serum albumin (BSA) due to its extensive use in the literature*(17, 28, 32, 36)* as well as its use to block the PVDF membrane. In a control sample without antibodies, AuNPs were incubated with BSA and exposed to a PVDF membrane containing immobilized lysozyme (LYZ). **Figure 3.6 A, B, C** show that during passivation, the LSPR of AuNPs shifted towards longer wavelength, while maintaining its deep red color. The highest shift was seen at 0.8 % BSA concentration with 2.0 nm and 4.0 nm shifts in water in TBST, respectively, indicating interactions between BSA and the AuNPs forming BSA coated gold nanoparticles (Au@BSA NP). However, this increase in LSPR shift seemed to plateau above BSA concentrations of 0.8 % where the shift deceased down to 1.0 nm in water and 3.0 nm in TBST (**Figure 3.6 B**). The variance in LSPR shift can be attributed to the exposure of AuNP to the buffer, but the changes in LSPR were approximately the same above 0.8% BSA.

When Au@BSA NP were incubated with the antigen, a band was shown where the lysozyme had been immobilized, indicating that Au@BSA NP is still able to attach to LYZ (**Figure 3.6 D**). The lack of passivation was observed across all concentrations of BSA (0.2 % to 1.4 %). Although the LYZ band thickness was slightly smaller in the 1.1 % BSA passivation compared to the others, an increase in passivating power was not observed with an increase in passivating BSA concentrations. As all bands shown in **Figure 3.6 D** have significant false positive results, BSA was deemed to not be an appropriate passivating agent in TBST.

Alternative passivating agents were also considered, including denatured BSA (dBSA), mercaptohexadecanoic acid (MHA), polyvinylpyrrolidone (PVP), and polyethylene glycol (PEG) with passivating times, 15 min, 3 h, and 24 h (**Figure 3.7**). In

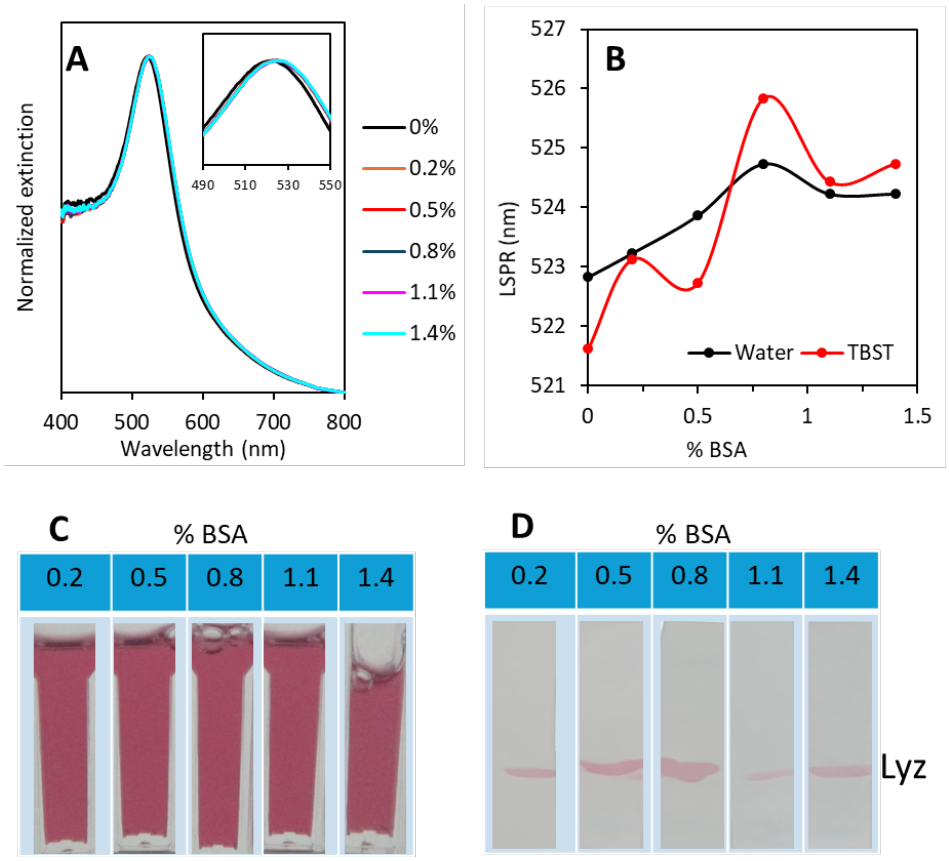

Figure 3.6. Passivation effect on optical properties of AuNP. *(A) Extinction spectra, (B) LSPR shift, and (C) photograph of AuNPs passivated with BSA in TBST buffer. (D) Photograph of PVDF membrane with immobilized Lysozyme (LYZ) after incubation with Au@BSA NP.*

addition to Lysozyme (LYZ), ovalbumin (OVA) was also immobilized on the PVDF membrane. **Figure 3.7** (top left) shows that with dBSA, the AuNP's LSPR shift around 6 nm toward longer wavelengths with no increase in the shift as the passivation time was increased. This indicates interactions between the dBSA and the AuNPs, forming dBSA coated gold nanoparticles (Au@dBSA NP). Incubation with MHA, PVP, or PEG resulted in shift of the LSPR towards shorter wavelengths regardless of concentration of passivating agents, suggesting that the passivating agents were not binding to AuNPs, and instead the nanoparticles were etching away.

The lack of a LSPR shift toward longer wavelength as an indicator for the lack of passivation, was confirmed on a blot with lysozyme immobilized on a PVDF membrane (**Figure 3.8)**. Both PVP and PEG were not appropriate passivating agents due to the positive bands showing especially in the OVA regardless of passivating time (**Figure 3.8, rows 3 and 4**). Compared to PVP and PEG, MHA seemed to perform better at passivating the AuNPs from the environment, however, this was only seen after passivation with 5 μM and 24 hour of passivation time (**Figure 3.8,** row 2). All other conditions showed red bands where the antigen (LYZ) and OVA were immobilized, indicating AuNPs aggregating to possibly the free thiol groups in the OVA and LYZ. When exposed to OVA and LYZ immobilized on PVDF membranes, the dBSA covered AuNPs demonstrated good passivation of against both proteins, making it a good candidate as a passivating agent. In all passivating times from 15 min to 24 hours and all concentrations of dBSA were strong candidates for passivation, as no band was observed (**Figure 3.8,** row 1).

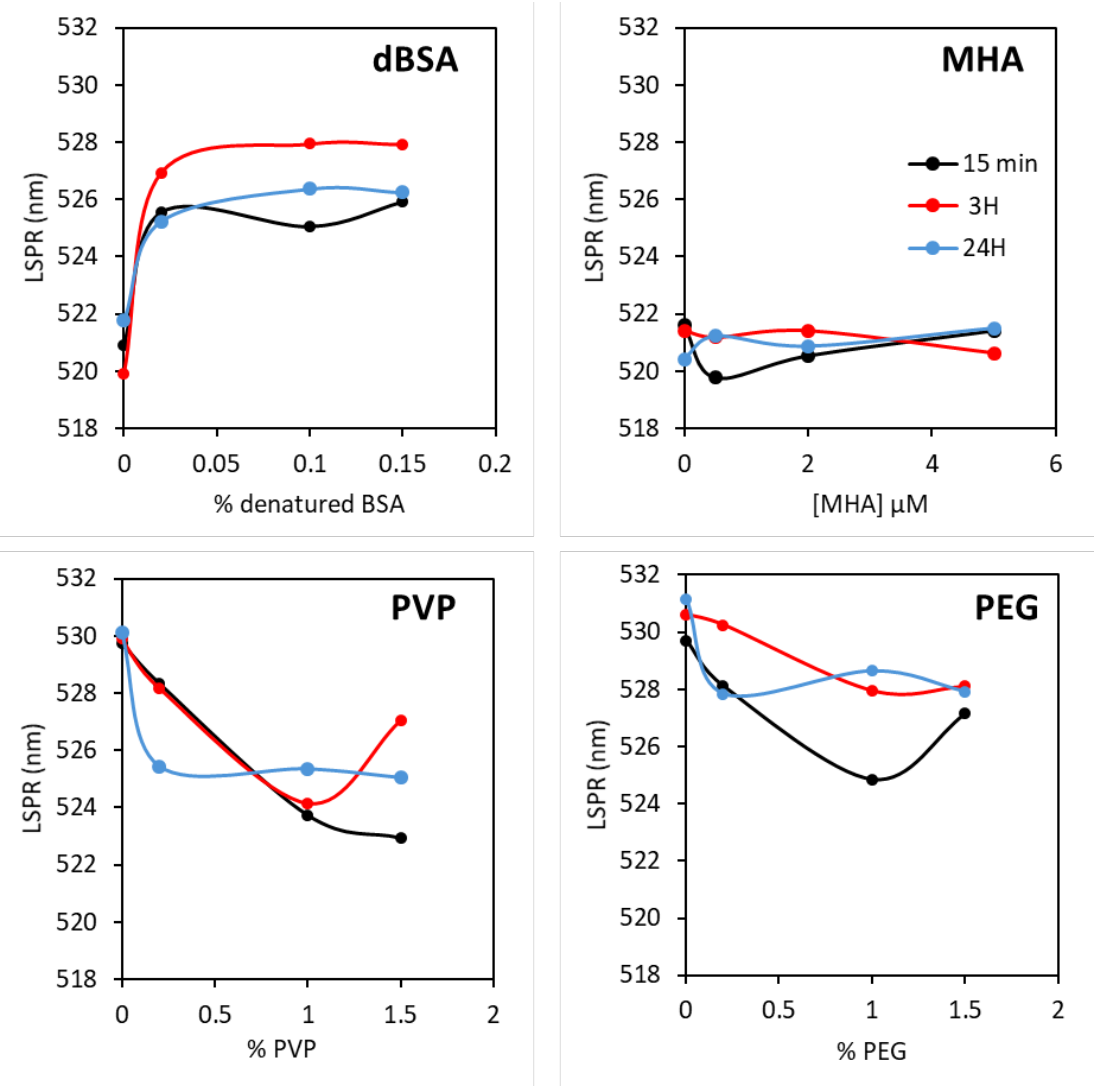

Figure 3.7. Effect of different passivating molecules on the LSPR of AuNP. *LSPR shift during passivation assay of AuNP with denature BSA (dBSA), mercaptohexadecanoic acid (MHA), polyvinylpyrrolidone (PVP), or polyethylene glycol (PEG) during 15 min (black), 3 hours (red) or 24 hours (blue).*

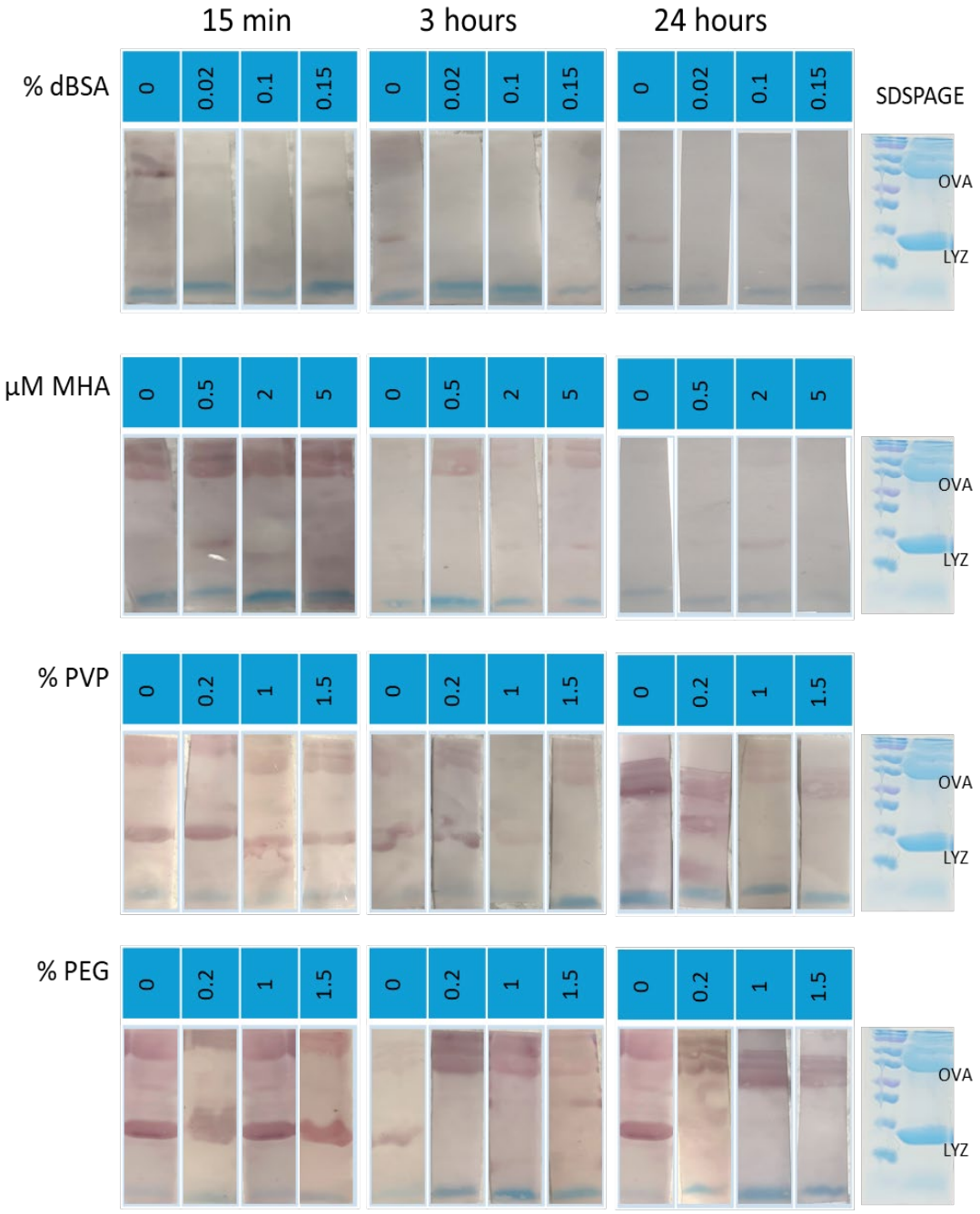

Figure 3.8. False positive results with different passivating molecules on Western blot. *Photographs of PVDF membranes after incubation for 15 min, 3 hours or 24 hours with AuNPs passivates with various concentrations of denatured BSA (dBSA), mercaptohexadecanoic acid (MHA), polyvinylpyrrolidone (PVP), or polyethylene glycol (PEG). Photograph at the far right is the matching SDSPAGE stained with Coomassie blue showing the protein ladder in the first lane and ovalbumin (OVA) and Lysozyme (LYZ) in the second lane. Membrane incubation was carried out in TBST buffer.*

Because dBSA was identified as a strong candidate as a passivating agent, a western blot was attempted with antibody tagged gold nanoparticle passivated with dBSA (Ab-Au@dBSA NP). **Figure 3.9** shows that without the antibody, the solution turns slightly blue, indicating that at 0.5 and 2 % dBSA the gold nanoparticles aggregate. This aggregation is not observed in the presence of antibody, demonstrating that the Ab-AuNP is more tolerant to high concentration of dBSA, regardless of passivation time. All these solutions were incubated with blots containing immobilized OVA and LYS using TBS buffer. In general, all blot showed a pink background, highlighting the lack of Tween 20 in the buffer. Different from the passivation at low concentration of dBSA in TBST buffer (**Figure 3.8** row 1), faint red bands of LYZ were observed for all blot including the controls without antibody; the bands were more intense when the passivation time was 24 h. As previously observed, OVA is not visualized when AuNP are passivated with dBSA.

In summary, BSA, PVP, MHA and PEG do not prevent the false positive obtained by the precipitation of AuNP on immobilized LYZ or OVA. The false positive was prevented at low concentration of dBSA, but observed at high concentrations of dBSA. Ab-AuNP is more stable in biochemical buffer than AuNP.

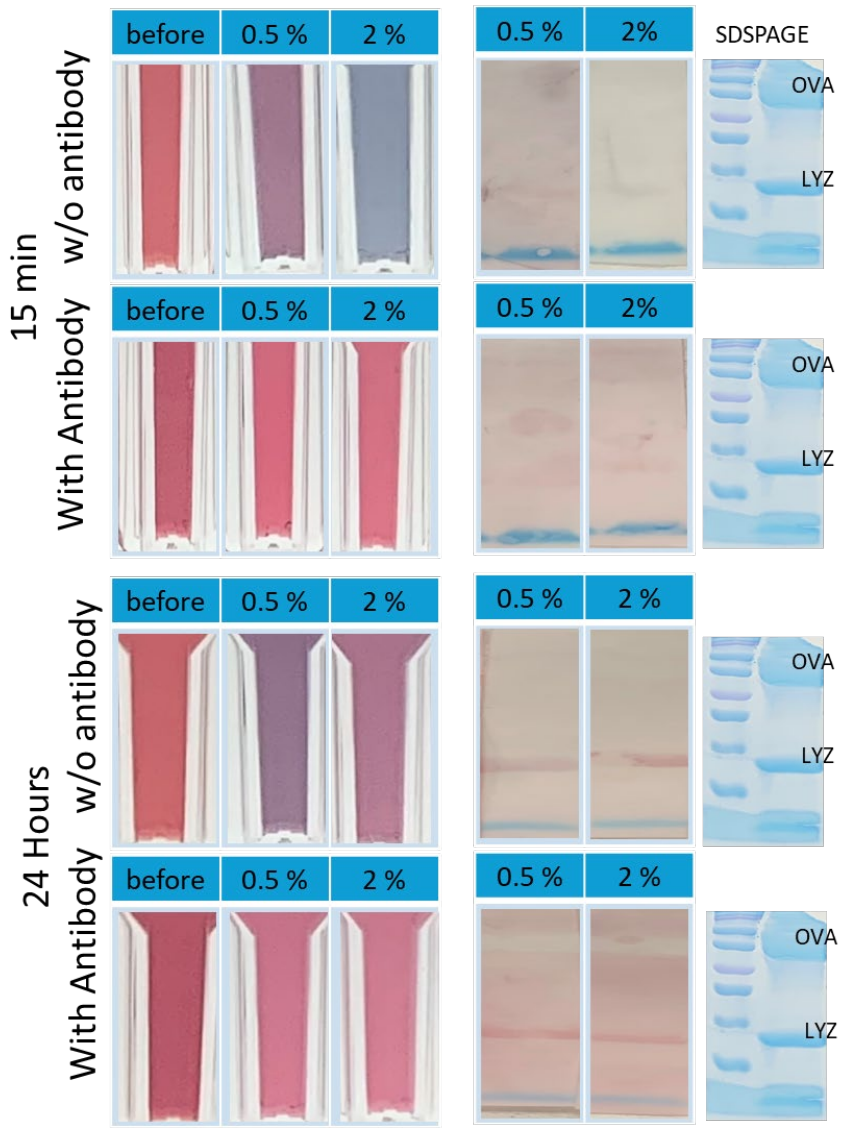

Figure 3.9. Effect of conjugation time and concentration of passivating agent on western blot. *(Left) Photograph of AuNPs with and without antibodies passivated with 0.5 or 2% dBSA for (top) 15 min or (bottom) 24 hours. (Right) Photographs of PVDF membranes after incubation with Au@dBSA. Photograph at the far right is the matching SDSPAGE stained with Coomassie blue showing the protein ladder in the first lane and ovalbumin (OVA) and Lysozyme (LYZ) in the second lane. Membrane incubation was carried out in TBS buffer.*

Section 3.5 Silver Nanoparticle Synthesis

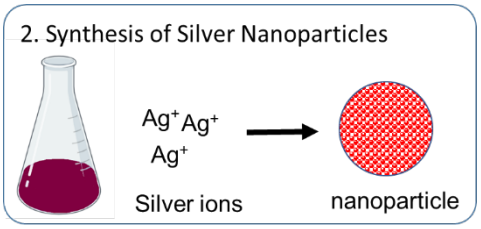

AgNP were synthesized by a modified work *(58)* of simultaneous multiple asymmetric reduction technique (SMART) as described by Mahmoud *(56)*. Nanoparticles prepared by this method enable high control over the anisotropic geometry of the AgNPs, where the L-ascorbic acid and sodium borohydride control the diameter and prism sharpness of the AgNP respectively *(56, 64)*.

UV-visible spectra and TEM micrograms (**Figure 3.10 C)** shows that nanoparticles have LSPR of 562 nm and average diameter of 30 ± 8 nm with thickness 8 ± 1 nm (**Figure 3.10 D and E**) observed in similar AgNP synthesis methods utilizing the ascorbic acid and borohydride reduction method *(56, 58)*. Although the color of the AgNP is not the same as the gold nanoparticle, the deep purple/blue color is also a desirable distinct color usable in western blot assays (**Figure 3.10 B**). Contrary to the large reproducibility of AuNP synthesis, AgNP vary greatly from batch to batch *(65)*, thus the color of AgNP solutions can vary from deep blue to slightly purple; for this reason, the analysis of AgNP is based on LSPR shift rather than absolute value. A theoretical concentration of 0.55 nM was calculated for silver nanoparticles using the dimensions of nanoparticles and amount of silver used in the reaction, assuming 100% formation of a perfect cylindrical nanoparticle. First, the total atoms of silver in the reaction were calculated knowing that the 100 mL of 0.18 mM silver solution was used each time.

$$total\ silver\ atoms = \ 0.18\ x10^{-3}\ \frac{mol\ Ag}{L} * 0.1\ L * 6.022\ x\ 10^{23}\ \frac{Ag\ atoms}{mol\ Ag}$$

$$total\ silver\ atoms = 1.1\ x10^{19}\ Ag\ atoms$$

Second, the atoms of silver in a cylindrical nanoparticle (30 nm wide and 8 nm height) were obtained using the density of silver (1.049 x 10^{-20} g/nm^3), molar mass of silver (107.9 g/mol), and the volume of a cylinder = $\pi r^2 h$.

$$Volume\ of\ NP = \ \pi\left(\frac{30}{2} nm\right)^2\ 8\ nm = 5655\ nm^3$$

$$Silver\ atoms\ per\ NP = 5655\ nm^3 * \frac{1.049\ x\ 10^{-20}\ g}{nm^3} * \frac{mol}{107.9\ g} * 6.022\ x\ 10^{23}\ \frac{atoms}{mol}$$

$$Silver\ atoms\ per\ NP = 331{,}058\ Ag\ atoms/NP$$

Finally, the concentration of AgNP of the 100 mL solution is:

$$[AgNP] = \frac{1.1\ x10^{19}\ Ag\ atoms}{331058\ Ag\ \frac{atoms}{NP}} * \frac{mol\ NP}{6.022\ x\ 10^{23}\ NP} * \frac{1}{0.1\ L} = 5.5\ x10^{\ -10}\ M$$

$$[AgNP] = 0.55\ nM$$

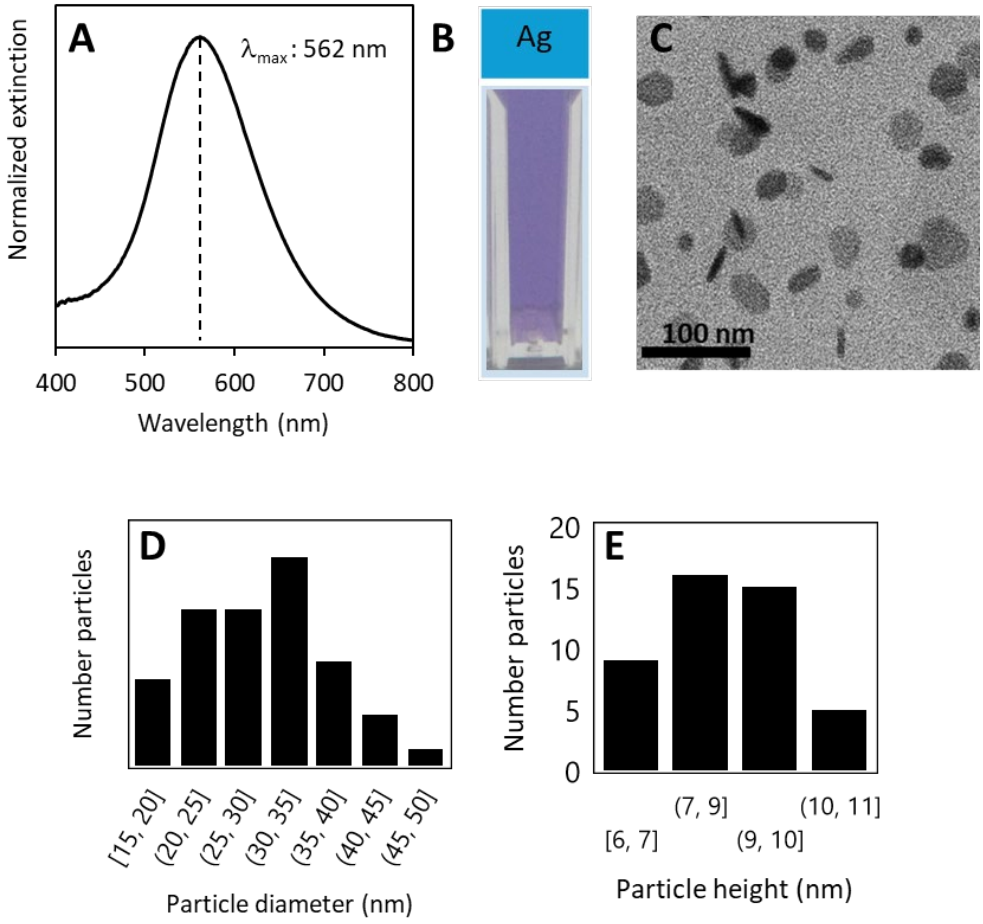

Figure 3.10. Characterization of AgNP. *(A) Extinction spectra, (B) photograph and (C) transmission electron micrographs of colloidal AuNP solution in water. Histograms showing nanoparticles have (D) average diameter of 30 ± 8 nm and (E) average height of 8 ± 1 nm (n = 45).*

Section 3.6 Silver Nanoparticle Conjugation

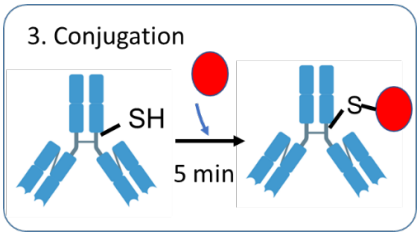

Changes in the optical properties of the nanoparticle correlate to changes in the environment shrouding the nanoparticles as observed with spherical AuNP; however, because AgNP are nanodisks these optical changes can also indicate reshaping of the nanoparticle from disk into spheres. **Figure 3.11** shows that the LSPR of AgNP did not shift upon a 3-minute conjugation with activated antibody. This lack of change in LSPR can be caused by the PVP molecules blocking the binding of Ab, compared to gold nanoparticles which were covered by citrate. However, when AgNP are centrifuged into BSA, the LSPR shifts towards longer wavelengths, suggesting the BSA can cover the nanoparticle without disturbing its structure, as structural changes to the nanoparticle will result in shift toward shorter wavelengths *(66)*. Similar to AuNP, conjugation of the antibody does not cause aggregation of AgNP. Because of the large affinity between sulfur and silver, conjugation is assumed even if LSPR shift was not recorded.

Section 3.7. Silver Nanoparticle stability

Binding between antibody and antigen occurs when these proteins have the correct charge and structure, which can be altered by pH and ion concentration, for these reasons, western blot is optimized for both specific binding conditions using a buffer and the addition of surfactants (Tween-20) to aid in removing background noise on the membrane.

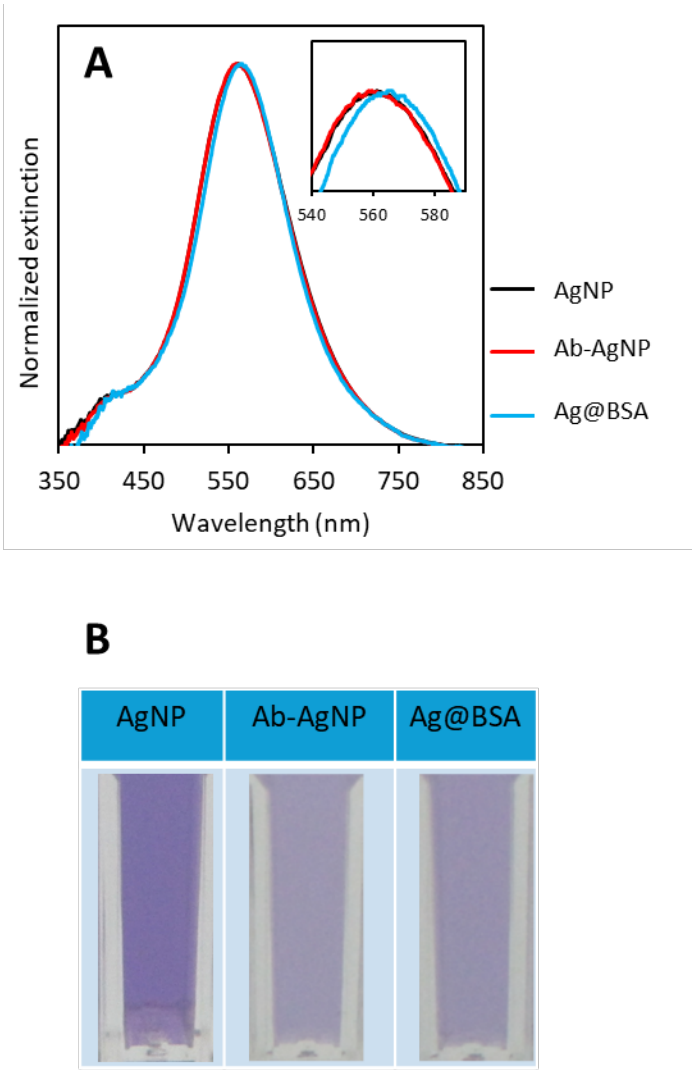

Figure 3.11. Conjugation with Antibody and passivation with BSA of AgNP. *(A) Extinction spectra and (B) photographs of AgNP in solution (Ag), conjugated with activated antibody (Ab-AgNP) and AgNP in BSA (Ag@BSA).*

Typical binding buffers used in western blot are TBST (50 mM Tris, 150 mM NaCl, 0.05 % Tween-20 pH 7.6), or PBST (3.2 mM Na_2HPO_4, 0.5 mM KH_2PO_4, 1.3 mM KCl, 135 mM NaCl, 0.05% Tween 20, pH 7.4). Compared to the geometrically stable spherical AuNPs, silver nanodisks could reshape if the stabilizing ligand molecules on its surface are altered. These western blot buffers can cause shape disruptions by displacing or changing the charges of the PVP or ascorbic acid on the surface of the nanoparticles. This section addresses the inferior stability of AgNP in biochemical buffers compared to AuNP. Centrifugation is used to exchange solvents.

In attempt to estimate the effect of biochemical buffers in the optical properties of AgNP, the AgNPs were introduced to tris-buffered saline (TBS pH 10.0), phosphate-buffered saline (PBS pH 7.2), TBS with tween 20 detergent (TBST pH 7.7), and PBS with tween 20 detergent (PBST pH 7.2). AgNP were introduced to buffer in two ways, either via centrifugation or dilution (without centrifugation). Via centrifugation, the nanoparticles are concentrated, and the supernatant with excess reagent molecules (PVP and citrate) are removed, then the nanoparticles are restored in buffer. Via dilution (without centrifugation), concentrated buffer is added to nanoparticles and excess reagents remain. The final concentrations of nanoparticles and buffer are the same in both approaches. **Figure 3.12 A** shows that when restored in water, the LSPR of the centrifuged AgNP shifts toward longer wavelength, while the dilution has almost no effect on the LSPR (**Figure 3.12 B**). The LSPR of the AgNP restored in all buffers shifted towards shorter wavelengths regardless of the method used to introduce the buffer.

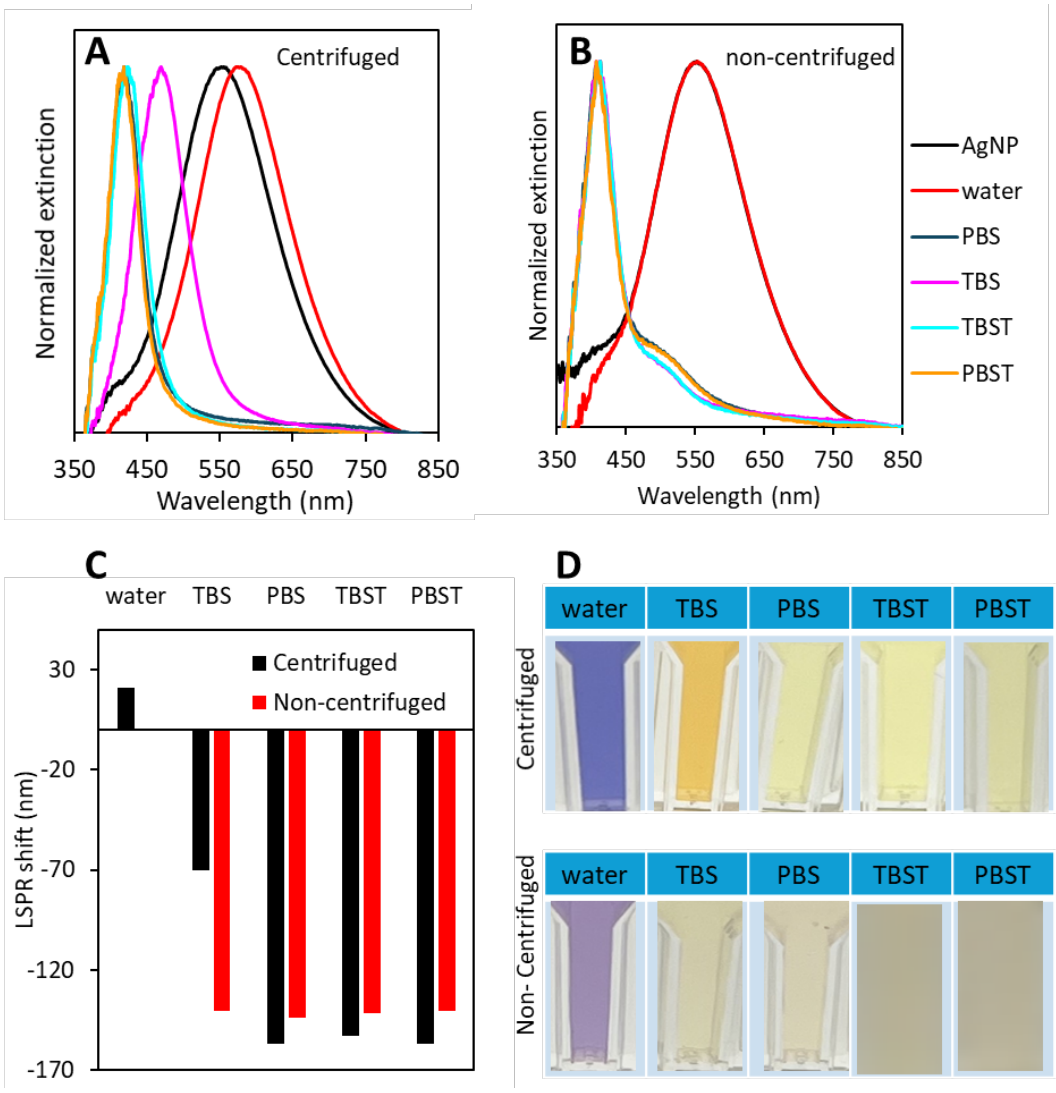

Figure 3.12. Effect of buffers nature and buffer exchange on the LSPR of AgNP. *Extinction spectra of AgNPs restored in water or buffer using (A) centrifugation or (B) just dilution. (C) Comparison of centrifugation effect on the LSPR shift and (D) photographs showing color change when AgNPs are restored in water or buffer. All measurements were done after 1 h.*

Centrifuged nanoparticles show a slightly larger shift which may be attributed to the removal of excess reagents in the solutions. Thus, centrifugation is deemed not necessary, and this step can be avoided for additional stabilization of AgNPs. Overall, there was no significant difference in change of LSPR caused by the Tris vs phosphate-based buffer (**Figure 3.12 C**). When comparing the change in LSPR by PBS and PBST, the presence of Tween does not seem to prevent the reshaping of nanoparticles and may only influence the western blot, removing background.

Figure 3.12 C shows that the LSPR shift at pH 10 (TBS buffer) is almost half of that observed at pH 7 (the rest of the buffers). Suggesting that at this high pH, it is more difficult to remove the PVP, thus reshape the nanoparticles. The main cause of shift is not a consequence of the nature of buffer (Tris vs. phosphate), the presence of detergent (Tween- 20) but is it more likely to be caused by the salt.

To further investigate, the possibility of NaCl in the biochemical buffers affecting the LSPR of the AgNPs was considered. At first, AgNPs were introduced to varying concentrations of NaCl from 150 mM to 3 mM of NaCl, as 150 mM is the concentration in the binding buffer. **Figure 3.13 A** shows that even in the lowest 3 mM concentration, the LSPR of the solution quickly changes. However, due to the realization of the possible role of the antibody as a passivating agent, the AgNP conjugated to antibodies (Ab-AgNPs) were also compared against the varying concentrations of NaCl. It must be noted that the assays with and without antibody were carried out with different batches of AgNP, thus the original color of the AgNP solutions is different. As observed before, conjugation with antibody did not caused an LSPR shift. **Figure 3.13 B** shows a decrease in LSPR shifts for Ab-AgNPs. A decrease in NaCl concentration as well as conjugation

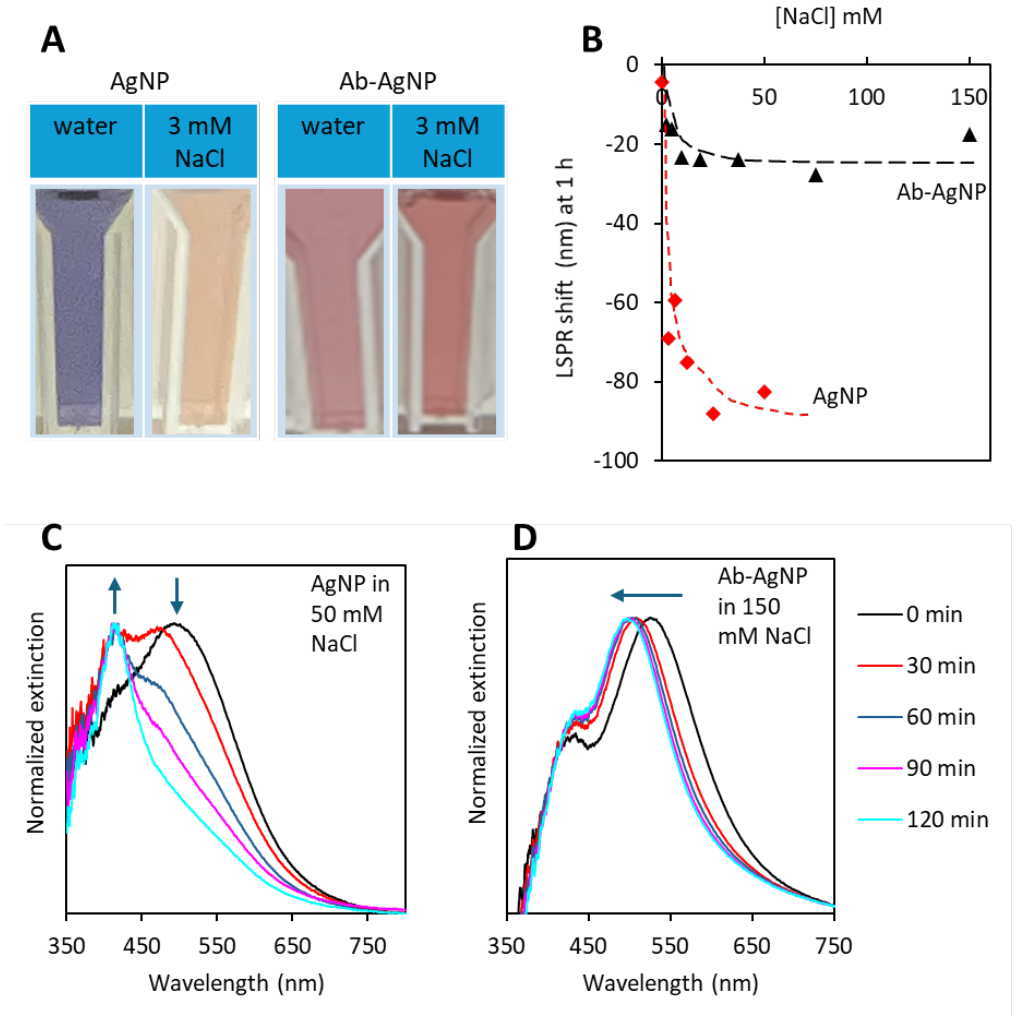

Figure 3.13. Effect of NaCl and antibody passivation on the LSPR of AgNP. *(A) Photographs of 1-hour old solutions of AgNP and AgAb conjugated nanoparticles in water or 3 mM NaCl. (B) Change in LSPR of AgNP (red dots) and AgNP conjugated to antibodies (black dots) over increasing concentrations of NaCl. Line has been added to guide the eye. Change in the extinction spectra for 2 h of (C) AgNP in 50 mM NaCl and (D) antibody conjugated AgNP in 150 mM NaCl. Assays with and without antibody were different batches, thus the initial color of solution is different.*

with antibodies can lower the LSPR shift caused by salt (**Figure 3.13 B**). The decrease in NaCl concentration was observed to decrease the LSPR shift by around 14 nm and with antibody conjugation the LSPR shift decreased by another 71 nm, keeping the AgNPs a red color, appropriate for western blot. The extinction spectra of both AgNP and Ab-AgNP show the resistance against an LSPR shift (**Figure 3.13 C, D**). After 15 mins of exposure to NaCl, bare AgNP show two LSPR peaks, one around 525 nm and another around 425 nm. The peak around 525 nm becomes smaller after 30 mins and becomes a "shoulder" with a smaller intensity and almost nonexistent after 1 hour. The large LSPR shift, approximately 150 nm, can be attributed to reshaping of nanoparticles into spheres *(66, 67)*. Spherical nanoparticles of silver are well known to be yellow in color with LSPR around 400 nm *(68)*. While the reshaping may not prevent the intended antibody binding in western blot, the yellow color does not offer adequate contrast to identify antigens against the white membrane of the western blot.

In summary, a dilution will suffice to transfer AgNP into buffer and centrifugation is not needed. The pH looks to affect the stability of the nanoparticles; however, this parameter is not flexible as most binding in western blot need a of pH 7. The major effect comes from the concentration of salt (NaCl) and the nature of the buffer (Tris or phosphate) or presence of detergent (Tween 20) does not seem to cause much difference. The conjugation of the antibody positively affects the stability of AgNP in biochemical buffer.

Section 3.8. Silver Nanoparticle Western blot.

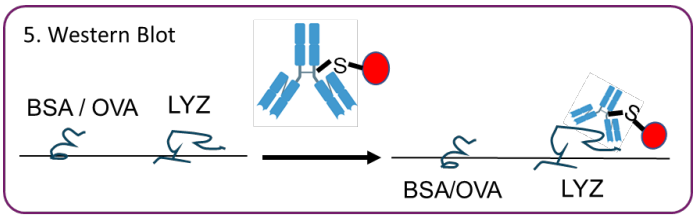

A western blot was attempted in water using AgNP and Ab-AgNP on a blot with immobilized OVA & LYZ or BSA & LYZ. **Figure 3.14** shows yellow bands for the lanes incubated with just bare AgNP, the AgNP presumably reshaped, showing the yellow band only bound to the antigen (LYZ) but not to BSA or OVA. Ab-AgNP produced the ideal darker lines of LYZ on the blot, especially during the longer 30 min conjugation. Ab-AgNP preserved its color, representing that the nanoparticles preserved their shape. The bare AgNP without any conjugation is only bound to LYZ and neither OVA nor BSA. This trend was seen throughout; AgNP and Ab-AgNP bound to only LYZ. Similar to the gold assay, the antibody labeled metal nanoparticle only binds to LYZ even in the presence of OVA.

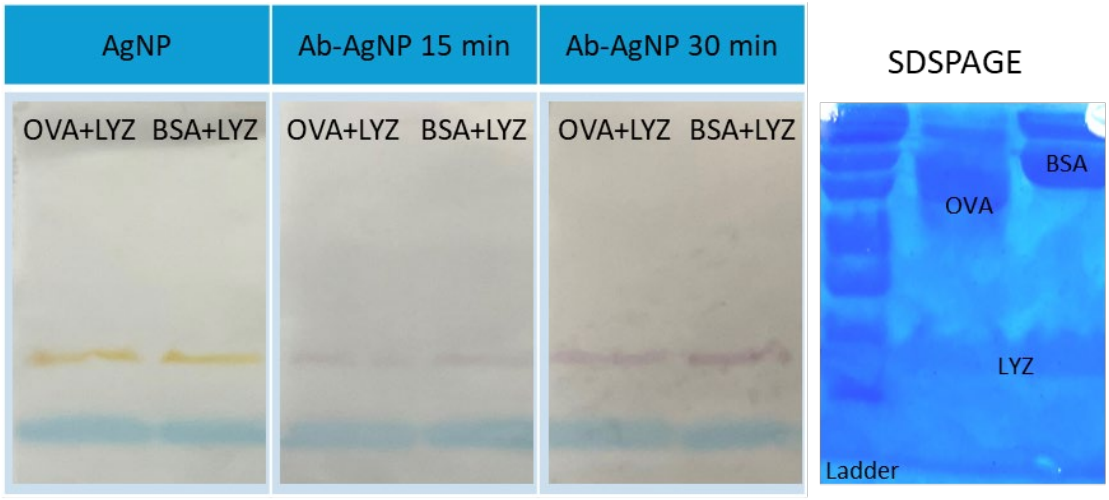

Figure 3.14. Western blot test with Ab labeled with AgNP. *Photographs of blots developed in TBST buffer using (left) bare AgNP, Ab-AgNP that were conjugated for (center) 15 min or (left) 30 min. The first lane of the blot has OVA and LYZ, while the second lane has BSA and LYZ. Photograph at the far right is the Coomassie blue stained SDSPAGE gel showing the relative positions of the protein ladder (first lane), OVA (second lane), and BSA (third lane). LYZ is shown in both second and third lanes. Membrane incubation was carried out in water.*

Chapter 4. DISCUSSION AND CONCLUSION

Section 4.1. Synthesis of antibody tagged with metal nanoparticle.

The objective of this work is to decrease the time of western blot by eliminating the need of a secondary antibody, which purpose is to provide a visual signal on the blot. Our strategy was to tag the primary antibody with a gold or silver nanoparticle (AuNP or AgNP), in which the tagged primary antibody offers both selectivity and visualization. In preparing the tagged antibody, it is important to consider time, cost, expertise needed, and preservation of color of the nanoparticles during the steps of western blot.

To conjugate the antibody to the metal nanoparticle, we took advantage of the high affinity between sulfur and metals. The Photochemical Immobilization Technique (PIT) produces free thiols on the antibody, as irradiation with 253.7 nm UV light for 1-minute selectively breaks dithiol bonds in the Fc region, and not in other parts of the antibody *(33)*. The Ellman's assay showed that warming up the lamp increased the concentration of free thiols (**Section 3.1**); a similar result was observed by other groups *(33, 35)*. Although the secondary antibody was used to validate free thiol formation, this result is consistent to the primary antibody as the thiol composition of the Fc region in antibodies is similar between antibodies. The large affinity of sulfur for metal nanoparticles the Fc region of the antibody binds to the metal nanoparticle, leaving the antigen biding site pointing outwards and in the correct orientation to recognize the antigen *(35, 36, 38)*.

The first advantage of PIT is the faster production of an antibody metal nanoparticle conjugate than other methods used to label antibodies. Activation of the antibody takes 1

min, and the conjugation between the activated antibody and the metal nanoparticle was achieved in approximately 15 min (**Figure 3.4**), bringing the total synthesis time to 16 min. In comparison, chemical activation of thiols in antibody can require 1 or 2 hours *(69)*, and chemical conjugation techniques used to label antibodies covalently to fluorescent molecules or enzymes like HRP take 2-3 hours and need purification steps and overnight dialysis *(70)*.

In an upper-level undergraduate teaching setting, producing an antibody tagged with metal nanoparticle using PIT is significantly safer, cheaper, and requires less expertise than other methods used to label antibodies. Although UV-light can be dangerous, this can be mitigated by using a metal cover. HRP labeling *(70)* and chemical activation of antibodies requires multiple steps *(69)*. For example, EDC/NHS coupling of nanoparticles and antibodies uses toxic EDC, which is not appropriate for a teaching setting. Thus, PIT is a facile synthesis method where only mixing and incubation is required, compared to organic synthesis and purification in other bonding methods. Because of both AuNP's and AgNP's facile synthesis and extensive use as biological contrasting agents, they are convenient and safe to use in an undergraduate teaching setting *(2, 7, 22, 24, 32)*. Regarding the cost, a labeling kit *(70)* for HRP is $750 which is much more compared to the cost of synthesis of AuNP and AgNPs.

Although color changes were observed in bare AuNP and AgNP (**Figure 3.5, 3.12, 3.13**), a metal nanoparticle conjugated with activated antibody preserved the color of nanoparticles wanted for western blot. During conjugation, the LSPR of nanoparticles shift up to 7 nm for AuNP (**Figure 3.4**) and no shift was observed for AgNP (**Figure 3.11**). As seen in **Figure 3.4**, AuNPs were seen to increase their LSPR slightly when exposed to UV

irradiated antibodies (LSPR shift < 10 nm). This small shift is representative of changes on the surface of the nanoparticles and does not indicate aggregation. Additionally, the lack of LSPR shift for AgNP in buffer suggest that PVP protects the nanoparticles *(71)*. The success of PIT is also confirmed by the positive LSPR shift of AuNPs during conjugation with the antibodies. To further confirm the antibody conjugation, comparisons of the measured LSPR shifts with the Rayleigh approximation, *(32)* refractive index, *(52)* size measurements with dynamic light scattering, *(7, 17)* and surface-enhanced Raman spectroscopy *(46, 72)* could be performed.

Section 4.2. Stability of antibody tagged with metal nanoparticle in solution.

Because the specific pH and ionic strength of the biochemical buffers provide optimal conditions for antibody-antigen binding on western blot, these conditions differ from the conditions in which metal nanoparticles are synthesized. Gold nanoparticles remain stable in solution solely by electrostatic repulsions of citrate ions covering the nanosphere *(16)*. The ascorbate and PVP allow silver nanodisks to remain in solution by electrostatic repulsions and to preserve their shape *(56, 59)*. Thus, exchanging nanoparticles into buffer can potentially cause their aggregation or reshaping if charged surface molecules are displaced by buffer or small ions like chloride.

Both AuNPs and AgNPs showed to be unstable in the biochemical buffer used for western blot; the major effect comes from the concentration of salt (NaCl) while the nature of the buffer (Tris or phosphate) or presence of detergent (Tween 20) does not seem to cause much difference (**Figures 3.5 and 3.12**). Aggregation can be avoided if the surface molecules cause enough steric hindrance to prevent nanoparticles from coming in contact

with each other. For this reason, most passivating agents are large polymeric molecules that can cause large hindrance. The small LSPR changes observed when AuNPs were passivated with low concentrations of BSA, dBSA, PVP, MHA, and PEG, indicate that these molecules can bind to the metal nanoparticle without causing aggregation *(28, 30, 32, 47-49)*. Both MHA and dBSA have thiol groups free to bind the metal nanoparticles. While dBSA seems to be a potential passivating agent, Au@dBSA NP crashed at high concentration (**Figure 3.9**). As seen in **Figure 3.12**, when exposed to NaCl, the LSPR shift of AgNPs was larger than 50 nm towards shorter wavelengths, implying reshaping of the silver nanodisks *(68)*. The major stabilization in solution was observed from the antibody itself, keeping a desirable dark color for the western blot (**Figures 3.9 and 3.13**). For further AgNP shape analysis during conjugation, surface-enhanced Raman spectroscopy, Fourier transform infrared spectroscopy, and atomic force microscopy *(73)* could be performed. In addition to the shape changes, these techniques could provide insight on the most affected capping agents causing the shape change and the role of the antibody against the AgNP reshaping.

Section 4.3. Western Blot with antibody tagged metal nanoparticle

For western blot to be effective and specific, non-specific bindings are undesirable; for instance, if the free surfaces of the metal nanoparticle conjugated to the antibody bind proteins on the membrane (blocking BSA and immobilized proteins), the whole membrane would be colored, making the antigen indistinguishable for the background. A false positive result would be found if the metal nanoparticle of the Ab-Au/Ag@dBSA binds to other immobilized proteins or if bare nanoparticle binds to the antigen (**Figure 4.1**).

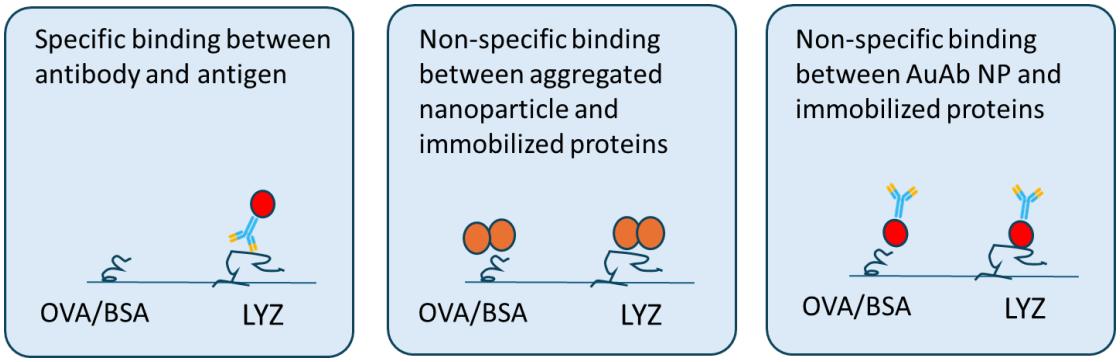

Figure 4.1 Specific and non-specific bindings to immobilized proteins in western blot.

When AuNP were passivated with BSA, a false positive of LYZ (the only immobilized protein) was observed (**Figure 3.6 D**) regardless of the concentration of passivating BSA. As seen in **Figure 3.8**, bare AuNPs and those passivated with MHA, PVP, or PEG showed bands for LYZ and/or immobilized ovalbumin (OVA), regardless of the concentration of passivating agents or passivation times. Only dBSA was able to passivate the surface of AuNP sufficiently to prevent non-specific binding of the bare nanoparticle (**Figure 3.8** row 1). Bare metal nanoparticles (electrostatically or sterically stable) are unlikely to bind to the PVDF membrane but could bind to the blocking BSA or immobilized proteins, especially if thiol groups are present. Because in SDS-PAGE the proteins are reduced and denatured before being resolved in the gel, it could be possible that immobilized proteins have exposed thiol groups, even if the oxidation of thiol groups, to form disulfide bonds, happens quickly.

Additionally, free thiol groups in the immobilized proteins could displace MHA, PVP, or PEG on the surface of AuNP, but cannot displace dBSA because this would bind to the surface of AuNP via similar thiol groups. False positive results were observed at high

concentrations of dBSA (**Figure 3.9** blots w/o antibody); this can of binding could be result of aggregation of AuNPs (**Figure 4.1**); however, the binding was only observed for LYZ and not OVA. Additionally, as shown in **Figure 3.9** row 4, the Ab-Au@dBSA NP seemed to avoid the membrane where the OVA resided. This could be due to the OVA having less exposed thiol groups per mass compared to LYZ (**Figures 3.9, 3.14**).

During the western blotting, both antibody conjugated nanoparticles were able to maintain a desirable deep red color as shown by the dark band at the position of immobilized lysozyme (**Figures 3.9, 3.14**), indicating that the antibodies were maintaining the AgNP and AuNP shapes, as bare nanoparticles were shown to aggregate or showed a slight color change in the AuNPs (**Figure 3.9** row 1, row 3) and showed to completely change color in AgNPs (**Figure 3.14**). These preliminary results show that both antibody conjugated AgNPs and AuNPs confer the visual detection capabilities to the primary antibody. For future examinations, surface-enhanced Raman spectroscopy *(28)*, and dynamic light scattering *(17)* could be employed to observe both the BSA and denatured BSA passivation with the nanoparticles.

Section 4.4. Conclusion

The synthesized gold and silver nanoparticles provide an alternative visualization solution for faster western blot. The feasibility of both gold and silver nanoparticles was demonstrated by the preservation of the deep red color during conjugation with antibodies (Section **3.3, 3.6**). Furthermore, the antibody increases the compatibility of AuNPs and AgNPs with western blot binding buffer. Passivation of the Ab-AuNP using low concentrations of dBSA eliminates false positives, and Ab-Au@dBSA NP only binds to

LYZ, as long as aggregation is avoided. However, the selectivity with AgNPs still need to be optimized. Similarly, the mechanisms in which Au@dBSA NP or bare AgNP selectively bind to LYZ but not to immobilized ovalbumin or BSA must be explored. By adding a tag on the primary antibody, downstream steps can be omitted, effectively allowing for a more streamlined western blot. Activation of antibody via PIT and conjugation are sufficiently short to represent an advantage over traditional western blot using an HRP-conjugated secondary antibody for visualization.

Acknowledgements

I thank Dr. Maryuri Roca for her unwavering support and advice throughout my undergraduate career in chemistry as well as the time in the research group. I would also like to thank Lily Kozel for the guidance and use of the Skidmore McGrow Microscopy Imaging Center, Lisa Quimby for the guidance and use of the Skidmore analytical interdisciplinary laboratory, and Dr. Madushi Raththagala for guidance and finalization on this work. I would like to thank the summer collaborative research fund for funding the research and support. Lastly, I would like to thank all my peers and my family who supported me throughout my 4 years at Skidmore.

TERMS AND ABBREVIATIONS

NP – Nanoparticle

AuNP – Gold nanoparticle

AgNP – Silver nanoparticle

LSPR – localized surface plasmon resonance

Ab – Antibody

Ab-AuNP– anti-lysozyme antibody tagged with gold nanoparticle

Ab-AgNP– anti-lysozyme antibody tagged with silver nanoparticle

Ab-Au@dBSA NP – anti-lysozyme antibody tagged with gold nanoparticle passivated with denatured BSA

PIT – Photochemical immobilization technique

BSA – Bovine Serum Albumin

dBSA – denatured Bovine Serum Albumin

PVP – polyvinylpyrrolidone

MHA – 6-mercaptohexadecanoic acid

LYZ – immobilized lysozyme

OVA – immobilized ovalbumin

REFERENCES

(1) Singh, P.; Pandit, S.; Mokkapati, V. R. S. S.; Garg, A.; Ravikumar, V.; Mijakovic, I. Gold Nanoparticles in Diagnostics and Therapeutics for Human Cancer. *International Journal of Molecular Sciences* **2018***, 19*, DOI: 10.3390/ijms19071979.

(2) Arruebo, M.; Valladares, M.; González-Fernández, Á Antibody-Conjugated Nanoparticles for Biomedical Applications. *Journal of Nanomaterials* **2009***, 2009*, 439389, DOI: 10.1155/2009/439389.

(3) Maher, S.; Kamel, M.; Demerdash, Z.; El Baz, H.; Sayyouh, O.; Saad, A.; Ali, N.; Salah, F.; Atta, S. Gold conjugated nanobodies in a signal-enhanced lateral flow test strip for rapid detection of SARS-CoV-2 S1 antigen in saliva samples. *Scientific Reports* **2023***, 13*, 10643, DOI: 10.1038/s41598-023-37347-y.

(4) Ardekani, L. S.; Thulstrup, P. W. Gold Nanoparticle-Mediated Lateral Flow Assays for Detection of Host Antibodies and COVID-19 Proteins. *Nanomaterials* **2022***, 12*, DOI: 10.3390/nano12091456.

(5) Wang, J.; Drelich, A. J.; Hopkins, C. M.; Mecozzi, S.; Li, L.; Kwon, G.; Hong, S. Gold nanoparticles in virus detection: Recent advances and potential considerations for SARS-CoV-2 testing development. *WIREs Nanomed Nanobiotechnol* **2022***, 14*, e1754, DOI: 10.1002/wnan.1754.

(6) Ventura, B. D.; Cennamo, M.; Minopoli, A.; Campanile, R.; Censi, S. B.; Terracciano, D.; Portella, G.; Velotta, R. Colorimetric Test for Fast Detection of SARS-CoV-2 in Nasal and Throat Swabs. *ACS Sens.* **2020***, 5*, 3043-3048, DOI: 10.1021/acssensors.0c01742.

(7) Yen, C.; de Puig, H.; Tam, J. O.; Gómez-Márquez, J.; Bosch, I.; Hamad-Schifferli, K.; Gehrke, L. Multicolored silver nanoparticles for multiplexed disease diagnostics: distinguishing dengue, yellow fever, and Ebola viruses. *Lab Chip* **2015***, 15*, 1638-1641, DOI: 10.1039/C5LC00055F.

(8) Mahmood, T.; Yang, P. Western blot: technique, theory, and trouble shooting. *N. Am. J. Med. Sci.* **2012***, 4*, 429-434, DOI: 10.4103/1947-2714.100998.

(9) Kurien, B. T.; Scofield, R. H. Western blotting. *Methods* **2006***, 38*, 283-293, DOI: 10.1016/j.ymeth.2005.11.007.

(10) Ghosh, R.; Gilda, J., E.; Gomes, A.,V. The necessity of and strategies for improving confidence in the accuracy of western blots. *Expert Review of Proteomics* **2014***, 11*, 549-560, DOI: 10.1586/14789450.2014.939635.

(11) Lloyd, V. K.; Hawkins, R. G. Under-Detection of Lyme Disease in Canada. *Healthcare* **2018***, 6*, DOI: 10.3390/healthcare6040125.

(12) Alexander Thomas, S. Human Immunodeficiency Virus Diagnostic Testing: 30 Years of Evolution. *Clinical and Vaccine Immunology* **2016***, 23*, 249-253, DOI: 10.1128/CVI.00053-16.

(13) Sanchis-Gual, R.; Coronado-Puchau, M.; Mallah, T.; Coronado, E. Hybrid nanostructures based on gold nanoparticles and functional coordination polymers: Chemistry, physics and applications in biomedicine, catalysis and magnetism. *Coord. Chem. Rev.* **2023***, 480*, 215025, DOI: 10.1016/j.ccr.2023.215025.

(14) Willets, K. A.; Van Duyne, R. P. Y. 2. Localized Surface Plasmon Resonance Spectroscopy and Sensing. *Annual Review of Physical Chemistry, , 58*, 267-297, DOI: 10.1146/annurev.physchem.58.032806.104607.

(15) Petryayeva, E.; Krull, U. J. Localized surface plasmon resonance: Nanostructures, bioassays and biosensing—A review. *Anal. Chim. Acta* **2011***, 706*, 8-24, DOI: 10.1016/j.aca.2011.08.020.

(16) Roca, M.; Pandya, N. H.; Nath, S.; Haes, A. J. Linear Assembly of Gold Nanoparticle Clusters via Centrifugation. *Langmuir* **2010***, 26*, 2035-2041, DOI: 10.1021/la902572m.

(17) Ventura, B. D.; Cennamo, M.; Minopoli, A.; Campanile, R.; Censi, S. B.; Terracciano, D.; Portella, G.; Velotta, R. Colorimetric Test for Fast Detection of SARS-CoV-2 in Nasal and Throat Swabs. *ACS Sens.* **2020***, 5*, 3043-3048, DOI: 10.1021/acssensors.0c01742.

(18) Wang, J.; Drelich, A. J.; Hopkins, C. M.; Mecozzi, S.; Li, L.; Kwon, G.; Hong, S. Gold nanoparticles in virus detection: Recent advances and potential considerations for SARS-CoV-2 testing development. *WIREs Nanomed Nanobiotechnol* **2022***, 14*, e1754, DOI: 10.1002/wnan.1754.

(19) Ardekani, L. S.; Thulstrup, P. W. Gold Nanoparticle-Mediated Lateral Flow Assays for Detection of Host Antibodies and COVID-19 Proteins. *Nanomaterials* **2022***, 12*, DOI: 10.3390/nano12091456.

(20) Maher, S.; Kamel, M.; Demerdash, Z.; El Baz, H.; Sayyouh, O.; Saad, A.; Ali, N.; Salah, F.; Atta, S. Gold conjugated nanobodies in a signal-enhanced lateral flow test strip for rapid detection of SARS-CoV-2 S1 antigen in saliva samples. *Scientific Reports* **2023***, 13*, 10643, DOI: 10.1038/s41598-023-37347-y.

(21) El-Sayed, I. H.; Huang, X.; El-Sayed, M. A. Selective laser photo-thermal therapy of epithelial carcinoma using anti-EGFR antibody conjugated gold nanoparticles. *Cancer Lett.* **2006***, 239*, 129-135, DOI: 10.1016/j.canlet.2005.07.035.

(22) Liu, X.; Dai, Q.; Austin, L.; Coutts, J.; Knowles, G.; Zou, J.; Chen, H.; Huo, Q. A One-Step Homogeneous Immunoassay for Cancer Biomarker Detection Using Gold Nanoparticle Probes Coupled with Dynamic Light Scattering. *J. Am. Chem. Soc.* **2008***, 130*, 2780-2782, DOI: 10.1021/ja711298b.

(23) Singh, P.; Pandit, S.; Mokkapati, V. R. S. S.; Garg, A.; Ravikumar, V.; Mijakovic, I. Gold Nanoparticles in Diagnostics and Therapeutics for Human Cancer. *International Journal of Molecular Sciences* **2018***, 19*, DOI: 10.3390/ijms19071979.

(24) Hirsch, L. R.; Jackson, J. B.; Lee, A.; Halas, N. J.; West, J. L. A Whole Blood Immunoassay Using Gold Nanoshells. *Anal. Chem.* **2003***, 75*, 2377-2381, DOI: 10.1021/ac0262210.

(25) Calderón-Jiménez, B.; Johnson, M. E.; Montoro Bustos, A. R.; Murphy, K. E.; Winchester, M. R.; Vega Baudrit, J. R. Silver Nanoparticles: Technological Advances, Societal Impacts, and Metrological Challenges. *Frontiers in Chemistry* **2017***, 5*.

(26) Quesada-González, D.; Merkoçi, A. Nanomaterial-based devices for point-of-care diagnostic applications. *Chem. Soc. Rev.* **2018***, 47*, 4697-4709, DOI: 10.1039/C7CS00837F.

(27) Zhang, L.; Mazouzi, Y.; Salmain, M.; Liedberg, B.; Boujday, S. Antibody-Gold Nanoparticle Bioconjugates for Biosensors: Synthesis, Characterization and Selected Applications. *Biosensors and Bioelectronics* **2020***, 165*, 112370, DOI: 10.1016/j.bios.2020.112370.

(28) Mustafaoglu, N.; Kiziltepe, T.; Bilgicer, B. Site-specific conjugation of an antibody on a gold nanoparticle surface for one-step diagnosis of prostate specific antigen with dynamic light scattering. *Nanoscale* **2017***, 9*, 8684-8694, DOI: 10.1039/C7NR03096G.

(29) Welch, N. G.; Scoble, J. A.; Muir, B. W.; Pigram, P. J. Orientation and characterization of immobilized antibodies for improved immunoassays (Review). *Biointerphases* **2017***, 12*, 02D301, DOI: 10.1116/1.4978435.

(30) Oliveira, J. P.; Prado, A. R.; Keijok, W. J.; Antunes, P. W. P.; Yapuchura, E. R.; Guimarães, M.,Cesar Cunegundes Impact of conjugation strategies for targeting of antibodies in gold nanoparticles for ultrasensitive detection of 17β-estradiol. *Scientific Reports* **2019***, 9*, 13859, DOI: 10.1038/s41598-019-50424-5.

(31) Sokolov, K.; Follen, M.; Aaron, J.; Pavlova, I.; Malpica, A.; Lotan, R.; Richards-Kortum, R. Real-Time Vital Optical Imaging of Precancer Using Anti-Epidermal Growth Factor Receptor Antibodies Conjugated to Gold Nanoparticles1. *Cancer Res.* **2003***, 63*, 1999-2004.

(32) Iarossi, M.; Schiattarella, C.; Rea, I.; De Stefano, L.; Fittipaldi, R.; Vecchione, A.; Velotta, R.; Ventura, B. D. Colorimetric Immunosensor by Aggregation of Photochemically Functionalized Gold Nanoparticles. *ACS Omega* **2018***, 3*, 3805-3812, DOI: 10.1021/acsomega.8b00265.

(33) Neves-Petersen, M.; Snabe, T.; Klitgaard, S.; Duroux, M.; Petersen, S. B. Photonic activation of disulfide bridges achieves oriented protein immobilization on biosensor surfaces. *Protein Science* **2006***, 15*, 343-351, DOI: 10.1110/ps.051885306.

(34) Wongkongkathep, P.; Li, H.; Zhang, X.; Ogorzalek Loo, R. R.; Julian, R. R.; Loo, J. A. Enhancing protein disulfide bond cleavage by UV excitation and electron capture

dissociation for top-down mass spectrometry. *International Journal of Mass Spectrometry* **2015***, 390*, 137-145, DOI: 10.1016/j.ijms.2015.07.008.

(35) Della Ventura, B.; Schiavo, L.; Altucci, C.; Esposito, R.; Velotta, R. Light assisted antibody immobilization for bio-sensing. *Biomed. Opt. Express* **2011***, 2*, 3223-3231, DOI: 10.1364/BOE.2.003223.

(36) Della Ventura, B.; Iannaccone, M.; Funari, R.; Pica Ciamarra, M.; Altucci, C.; Capparelli, R.; Roperto, S.; Velotta, R. Effective antibodies immobilization and functionalized nanoparticles in a quartz-crystal microbalance-based immunosensor for the detection of parathion. *PLoS One* **2017***, 12*, e0171754, DOI: 10.1371/journal.pone.0171754.

(37) Della Ventura, B.; Sakač, N.; Funari, R.; Velotta, R. Flexible immunosensor for the detection of salivary α-amylase in body fluids. *Talanta* **2017***, 174*, 52-58, DOI: 10.1016/j.talanta.2017.05.075.

(38) Cimafonte, M.; Fulgione, A.; Gaglione, R.; Papaianni, M.; Capparelli, R.; Arciello, A.; Bolletti Censi, S.; Borriello, G.; Velotta, R.; Della Ventura, B. Screen Printed Based Impedimetric Immunosensor for Rapid Detection of Escherichia coli in Drinking Water. *Sensors* **2020***, 20*, DOI: 10.3390/s20010274.

(39) Funari, R.; Della Ventura, B.; Altucci, C.; Offenhäusser, A.; Mayer, D.; Velotta, R. Single Molecule Characterization of UV-Activated Antibodies on Gold by Atomic Force Microscopy. *Langmuir* **2016***, 32*, 8084-8091, DOI: 10.1021/acs.langmuir.6b02218.

(40) Funari, R.; Della Ventura, B.; Carrieri, R.; Morra, L.; Lahoz, E.; Gesuele, F.; Altucci, C.; Velotta, R. Detection of parathion and patulin by quartz-crystal microbalance functionalized by the photonics immobilization technique. *Biosensors and Bioelectronics* **2015***, 67*, 224-229, DOI: 10.1016/j.bios.2014.08.020.

(41) Funari, R.; Della Ventura, B.; Schiavo, L.; Esposito, R.; Altucci, C.; Velotta, R. Detection of Parathion Pesticide by Quartz Crystal Microbalance Functionalized with UV-Activated Antibodies. *Anal. Chem.* **2013***, 85*, 6392-6397, DOI: 10.1021/ac400852c.

(42) Fulgione, A.; Cimafonte, M.; Della Ventura, B.; Iannaccone, M.; Ambrosino, C.; Capuano, F.; Proroga, Y. T. R.; Velotta, R.; Capparelli, R. QCM-based immunosensor for rapid detection of Salmonella Typhimurium in food. *Scientific Reports* **2018***, 8*, 16137, DOI: 10.1038/s41598-018-34285-y.

(43) AU - Higashi, S.,L.; AU - Yagyu, K.; AU - Nagase, H.; AU - Pearson, C.,S.; AU - Geller, H.,M.; AU - Katagiri, Y. Ultra-High-Speed Western Blot using Immunoreaction Enhancing Technology. *JoVE* **2020**, e61657, DOI: 10.3791/61657.

(44) Bergendahl, V.; Glaser, B. T.; Burgess, R. R. A fast Western blot procedure improved for quantitative analysis by direct fluorescence labeling of primary antibodies. *J. Immunol. Methods* **2003***, 277*, 117-125, DOI: 10.1016/S0022-1759(03)00183-2.

(45) Buchwalow, I. B.; Böcker, W. In *Antibody Labeling and the Choice of the Label;* Buchwalow, I. B., Böcker, W., Eds.; Immunohistochemistry: Basics and Methods; Springer Berlin Heidelberg: Berlin, Heidelberg, 2010; pp 9-17.

(46) Cui, Y.; Ren, B.; Yao, J.; Gu, R.; Tian, Z. Synthesis of AgcoreAushell Bimetallic Nanoparticles for Immunoassay Based on Surface-Enhanced Raman Spectroscopy. *J Phys Chem B* **2006***, 110*, 4002-4006, DOI: 10.1021/jp056203x.

(47) Radziuk, D.; Skirtach, A.; Sukhorukov, G.; Shchukin, D.; Möhwald, H. Stabilization of Silver Nanoparticles by Polyelectrolytes and Poly(ethylene glycol). *Macromol. Rapid Commun.* **2007***, 28*, 848-855, DOI: 10.1002/marc.200600895.

(48) Louie, S. M.; Gorham, J. M.; Tan, J.; Hackley, V. A. Ultraviolet photo-oxidation of polyvinylpyrrolidone (PVP) coatings on gold nanoparticles. *Environ. Sci. : Nano* **2017***, 4*, 1866-1875, DOI: 10.1039/C7EN00411G.

(49) Gupta, R. K.; Srinivasan, M. P.; Dharmarajan, R. Synthesis of 16-Mercaptohexadecanoic acid capped gold nanoparticles and their immobilization on a substrate. *Mater Lett* **2012***, 67*, 315-319, DOI: 10.1016/j.matlet.2011.09.047.

(50) Riddles, P. W.; Blakeley, R. L.; Zerner, B. Ellman's reagent: 5,5′-dithiobis(2-nitrobenzoic acid)—a reexamination. *Anal. Biochem.* **1979***, 94*, 75-81, DOI: 10.1016/0003-2697(79)90792-9.

(51) Riddles, P. W.; Blakeley, R. L.; Zerner, B. [8] Reassessment of Ellman's reagent. *Meth. Enzymol.* **1983***, 91*, 49-60, DOI: 10.1016/S0076-6879(83)91010-8.

(52) Danischewski, J.; Donelson, D.; Farzansyed, M.; Jacoski, E.; Kato, H.; Lucin, Q.; Roca, M. Color Transferability from Solution to Solid Using Silica Coated Silver Nanoparticles. *Langmuir* **2023***, 39*, 1786-1792, DOI: 10.1021/acs.langmuir.2c02611.

(53) Grabar, K. C.; Freeman, R. G.; Hommer, M. B.; Natan, M. J. Preparation and Characterization of Au Colloid Monolayers. *Anal. Chem.* **1995***, 67*, 735-743, DOI: 10.1021/ac00100a008.

(54) Turkevich, J.; Stevenson, P. C.; Hillier, J. A study of the nucleation and growth processes in the synthesis of colloidal gold. *Discuss. Faraday Soc.* **1951***, 11*, 55-75, DOI: 10.1039/DF9511100055.

(55) FRENS, G. Controlled Nucleation for the Regulation of the Particle Size in Monodisperse Gold Suspensions. *Nature Physical Science* **1973***, 241*, 20-22, DOI: 10.1038/physci241020a0.

(56) Mahmoud, M. A. Simultaneous Reduction of Metal Ions by Multiple Reducing Agents Initiates the Asymmetric Growth of Metallic Nanocrystals. *Crystal Growth & Design* **2015***, 15*, 4279-4286, DOI: 10.1021/acs.cgd.5b00592.

(57) Haiss, W.; Thanh, N. T. K.; Aveyard, J.; Fernig, D. G. Determination of Size and Concentration of Gold Nanoparticles from UV−Vis Spectra. *Anal. Chem.* **2007***, 79*, 4215-4221, DOI: 10.1021/ac0702084.

(58) Danischewski, J. Preserving the color of silver nanoparticles from solution into PVA films using silica coatings , Skidmore College, 2021.

(59) Chen, H.; Kou, X.; Yang, Z.; Ni, W.; Wang, J. Shape- and Size-Dependent Refractive Index Sensitivity of Gold Nanoparticles. *Langmuir* **2008**, *24*, 5233-5237, DOI: 10.1021/la800305j.

(60) Haes, A. J.; Zou, S.; Schatz, G. C.; Van Duyne, R. P. A Nanoscale Optical Biosensor: The Long Range Distance Dependence of the Localized Surface Plasmon Resonance of Noble Metal Nanoparticles. *J Phys Chem B* **2004**, *108*, 109-116, DOI: 10.1021/jp0361327.

(61) BioRad Mini-PROTEAN Empty Cassette Gel Casting Instructions, Rev A 10024259. *https://www.bio-rad.com/sites/default/files/webroot/web/pdf/lsr/literature/10024259.pdf*.

(62) ThermoScientific Ellman's Reagent Assay 22582 . *https://www.thermofisher.com/document-connect/document-connect.html?url=https://assets.thermofisher.com/TFS-Assets%2FLSG%2Fmanuals%2FMAN0011216_Ellmans_Reag_UG.pdf*.

(63) Njoki, P. N.; Lim, I.; Mott, D.; Park, H.; Khan, B.; Mishra, S.; Sujakumar, R.; Luo, J.; Zhong, C. Size Correlation of Optical and Spectroscopic Properties for Gold Nanoparticles. *J. Phys. Chem. C* **2007**, *111*, 14664-14669, DOI: 10.1021/jp074902z.

(64) Métraux, G.; Mirkin, C. Rapid Thermal Synthesis of Silver Nanoprisms with Chemically Tailorable Thickness. *Adv Mater* **2005**, *17*, 412-415, DOI: 10.1002/adma.200401086.

(65) Horne, J.; De Bleye, C.; Lebrun, P.; Kemik, K.; Van Laethem, T.; Sacré, P.; Hubert, P.; Hubert, C.; Ziemons, E. Optimization of silver nanoparticles synthesis by chemical reduction to enhance SERS quantitative performances: Early characterization using the quality by design approach. *J. Pharm. Biomed. Anal.* **2023**, *233*, 115475, DOI: 10.1016/j.jpba.2023.115475.

(66) Kelly, K. L.; Coronado, E.; Zhao, L. L.; Schatz, G. C. The Optical Properties of Metal Nanoparticles: The Influence of Size, Shape, and Dielectric Environment. *J Phys Chem B* **2003**, *107*, 668-677, DOI: 10.1021/jp026731y.

(67) Lee, K.; El-Sayed, M. Gold and Silver Nanoparticles in Sensing and Imaging: Sensitivity of Plasmon Response to Size, Shape, and Metal Composition. *J Phys Chem B* **2006**, *110*, 19220-19225, DOI: 10.1021/jp062536y.

(68) Evanoff Jr., D. D.; Chumanov, G. Synthesis and Optical Properties of Silver Nanoparticles and Arrays. *ChemPhysChem* **2005**, *6*, 1221-1231, DOI: 10.1002/cphc.200500113.

(69) Wang, X.; Mei, Z.; Wang, Y.; Tang, L. Comparison of four methods for the biofunctionalization of gold nanorods by the introduction of sulfhydryl groups to antibodies. *Beilstein J. Nanotechnol* **2017**, *8*, 372-380, DOI: 10.3762/bjnano.8.39.

(70) Roche Peroxidase Labeling Kit
from horseradish # 11 829 696 001.
https://www.sigmaaldrich.com/deepweb/assets/sigmaaldrich/product/documents/127/842/11829696001.pdf.

(71) Madkour, M.; Bumajdad, A.; Al-Sagheer, F. To what extent do polymeric stabilizers affect nanoparticles characteristics? *Adv. Colloid Interface Sci.* **2019***, 270*, 38-53, DOI: 10.1016/j.cis.2019.05.004.

(72) Faried, M.; Suga, K.; Okamoto, Y.; Shameli, K.; Miyake, M.; Umakoshi, H. Membrane Surface-Enhanced Raman Spectroscopy for Cholesterol-Modified Lipid Systems: Effect of Gold Nanoparticle Size. *ACS Omega* **2019***, 4*, 13687-13695, DOI: 10.1021/acsomega.9b01073.

(73) Ahmed, D.; Raza, M.; Perveen, S.; Ahmed, S. Cephradine Coated Silver Nanoparticle their Drug Release Mechanism, and Antimicrobial Potential against Gram-Positive and Gram-Negative Bacterial Strains through AFM. *Journal-Chemical Society of Pakistan* **2018***, 40*.